INVESTIGATING AND MODELING THE ACOUSTIC RELEASE OF DOXORUBICIN FROM FOLATE-TARGETED MICELLES

by

Laura Kherbeck

A Thesis Presented to the Faculty of the
American University of Sharjah
College of Engineering
in Partial Fulfillment
of the Requirements
for the Degree of

Master of Science in
Chemical Engineering

Sharjah, United Arab Emirates

June 2012

Approval Signatures

We, the undersigned, approve the Master's Thesis of Laura Kherbeck.

Thesis Title: Investigating and Modeling the Acoustic Release of Doxorubicin from Folate-Targeted Micelles

Signature	**Date of Signature**
_____	_____
Dr. Ghaleb Al Husaini Associate Professor, Department of Chemical Engineering Thesis Advisor	
_____	_____
Dr. Nabil Abdel Jabbar Professor, Department of Chemical Engineering Thesis Committee Member	
_____	_____
Dr. Hasan Al-Nashash Professor, Department of Electrical Engineering Thesis Committee Member	
_____	_____
Dr. Dana Marie Abouelnasr Head, Department of Chemical Engineering	
_____	_____
Dr. Hany El Kadi Associate Dean, College of Engineering	
_____	_____
Dr. Yousef Al-Assaf Dean, College of Engineering	
_____	_____
Dr. Khaled Assaleh Director of Graduate Studies	

Acknowledgements

I would like to express my sincere gratitude to all those who helped in the making of this thesis. To my thesis advisor Dr. Ghaleb Al Husseini, this thesis would not have been possible had it not been for the vast amounts of experimental data you brought back from your sabbatical. Thank you for your tremendous help and guidance along the way and for giving me the opportunity to work with you. And most importantly, thank you for the chance to be on your publications.

I also appreciate the suggestions made by my thesis committee members, Dr. Nabil Abdel Jabbar and Dr. Hasan Al-Nashash – thank you for taking the time to give me your input. To the Chemical Engineering Department at AUS, you have all been wonderful to work with and I could not have asked for better mentors. And last but not least, I want to thank my beautiful family for giving me the world and expecting nothing in return.

Abstract

To minimize the adverse side effects of conventional chemotherapy, a targeted micellar drug carrier was investigated that retains hydrophobic drugs in its core and then releases the drug via ultrasound. This thesis reports the synthesis of Pluronic P105 micelles with folic acid conjugated to their surface and measures the percent drug release from folated versus non-folated micelles at 70 kHz and different acoustic power densities. The encapsulated drug is Doxorubicin (Dox). Two physical models and their corresponding mathematical representation are then used to fit the data. The zero-order release with first-order re-encapsulation showed the best fit to the kinetic data of this targeted micellar system. Additionally, the acoustic activation power density and Gibbs free energy were calculated for folated and non-targeted micelles. An artificial neural network (ANN) model is also developed in an attempt to model the dynamic release of Dox from both folated and non-folated micelles and its subsequent re-encapsulation under various ultrasonic power densities at 70 kHz. The analysis shows that folated micelles exhibit a higher percentage of ultrasonic drug release than non-folated micelles. This could be because the folic acid ligand compromises the structural integrity of the micelle. Furthermore, the data suggest an important role of transient cavitation in drug release due to the presence of a power density threshold.

Table of Contents

List of Tables

List of Figures

Chapter 1: Introduction

Conventional chemotherapy has always had copious drawbacks; therefore when it was discovered that chemotherapy drugs could be sequestered inside a nanocarrier that would release them only when and where needed, it was unanimously agreed that cancer research had taken a giant leap forward. Nanocarrier drug-delivery systems posed one major advantage over conventional chemotherapy: since the drug was to be released only at the tumor site where it was needed, healthy tissue was not affected by the adverse presence of the drug. The drug is then released from the nanocarrier upon the application of an external stimulus, one of the most common being low-intensity ultrasound. Ultrasound can be described as the ideal stimulus since, other than enabling the nanocarrier to release its chemotherapeutic contents, it is non-invasive, this resulting in minimal damage to skin and other surrounding tissue. Moreover, ultrasonic waves propagate deep into the body and can be accurately focused on the tumor site. However, by far the most important property of ultrasound is its synergistic effect on drug activity brought about by what is believed to be enhanced endocytotic drug uptake by the tumor cell.

The drug-delivery mechanism is simple. The chemotherapy drug is loaded into a nanocarrier, or a micelle, by the simple act of mixing. The micelles with the sequestered drug are then administered to the patient via an IV injection and are allowed to circulate throughout the body. In time, low-frequency ultrasound is applied to the tumor area only, thereby prompting the micelles to release their drug. When the ultrasound is turned off, the drug is re-encapsulated back into the carrier. However, micelles are not without disadvantages; they are prone to a short blood half-life. Blood proteins are adsorbed onto the surface of these nanocarriers which makes them susceptible to recognition by the macrophages of the mononuclear phagocyte system (MPS). To enhance the carriers' circulation time in the blood, the carrier surface is modified via the addition of polyethylene glycol (PEG). This is effective because when the micelles are tagged by leukocytes, the protein tag will cause the PEG chains to retreat closer to the hydrophobic

micellar core. This “retreat” is entropically favorable and causes the PEG chains to repel the tag. Without the protein tag, the liver will not be able to recognize the micelle and label it as an invader and the micelle will be able to circulate in the blood for a longer period of time.

Since the nanocarrier surface modified with (PEG) became standard practice, it opened the door to further surface manipulation to enhance tumor-fighting potential. It was desired to find certain surface ligands that would enable even more nanocarriers to be taken in by the tumor cell and subsequently release the drug inside their cytoplasm The only logical way to do this was to render the nanocarrier more “appealing” to the tumor cell, which, biologically speaking, could be achieved by conjugating nonantigenic ligands to the surface of the micelle. These targeted micelles can then bind to receptors on the surface of the tumor cells. Various tumors have since been found to overexpress receptors for the vitamin folic acid. Thus, it became viable to modify the carrier surface by attaching a folic acid molecule.

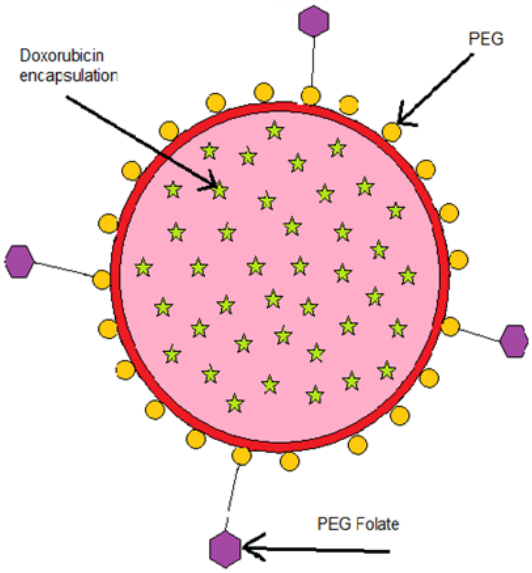

Figure 1. Schematic showing Dox encapsulated in a folated micelle

Once these targeted carriers are synthesized, it is essential to measure the amount of drug released from their core as compared to unfolated micelles and to study the mathematical mechanism by which the drug is released and subsequently re-encapsulated. To do so, it became necessary to develop models to attempt to describe release and re-encapsulation trends. It was also important to observe the influence of ultrasound power intensity on the percent drug release. This thesis reports the synthesis of Pluronic P105 micelles with folic acid conjugated to their surface and measures the percent drug release from folated versus unfolated micelles at different acoustic power densities. The encapsulated drug is Doxorubicin (Dox). Then, the fit of the release and re-encapsulation experimental data to two mathematical models is presented in an attempt to better understand the physical mechanisms involved. Finally, an artificial neural network (ANN) model is developed in an attempt to model the dynamic release of Dox from both folated and non-folated micelles and its subsequent re-encapsulation under various ultrasonic power densities at 70 kHz.

Chapter 2: Literature Review

2.1 Micelles

In the science of nanomedicine, one of the most useful modalities for efficient drug delivery is the micelle. Micelles are block copolymers that assemble themselves (self-assembly), with sizes ranging between 10 to 500 nm. They are characterized by their hydrophobic core and hydrophilic shell structure. The hydrophobic drug is loaded into the core, while the shell is usually poly(ethylene glycol) (PEG). Micelles display an advantage over other nanocarriers due to their easy method of preparation, the simplicity of drug loading into the core, their stability, and the fact that drug release from micelles can be controlled with relative ease. Micelles exhibit low critical micelle concentrations (CMC) which indicates their thermodynamic stability *in vitro* and *in vivo*. This stability does not allow for rapid dissociation, which is advantageous. Furthermore, micelles have a long circulation time in blood and their small size allows them to escape renal excretion, while successfully extravasating in the tumor [1].

Pluronic polymers are triblock copolymers of poly(ethylene oxide) (PEO) – poly(propylene oxide) (PPO)- poly(ethylene oxide) (PEO). They are water-soluble, and form micelles when concentrations are sufficiently high. The hydrophobic block forms the core of the micelle and the hydrophilic PEO chains form the corona. The result is a spherical core-shell structure [2].

Amphiphilic copolymer micelles are listed as some of the most important types of carriers for chemotherapy drugs. The drug is usually introduced into the biodegradable polymer matrix by mixing, and is slowly released upon the degradation of the matrix or by diffusing out of the polymer [3]. Of particular interest is poly (lactic acid)-b-poly (ethylene glycol) (PLA-b-PEG) since these micelles are biodegradable, biocompatible, and exhibit proper hydrophilicity (to allow for accumulation of the chemotherapy drug inside their core). Its degradation products are non-toxic and can be excreted by the kidneys [4]. Several methods of loading PLA shelled micelles with the drug doxorubicin have been tested [5].

Lipophilic drugs exhibit poor water solubility, which greatly restricts their clinical applications. For instance, the drug honokiol showed promise in cancer treatment and its potential could not be realized without the use of biodegradable polymeric nanoparticles which would be used as carriers for the drug injected via IV injection. A self-assembled monomethoxy poly(ethylene glycol)-poly(ε-caprolactone) (MPEG-PCL) diblock copolymeric micelle has been designed to overcome the hydrophobicity of this drug [6].

The problem with Pluronic P-105 micelles is their quick dissolution upon dilution. Significant dilution is inevitable when using IV injection [7]. The solution is to stabilize the micelles using an interpenetrating network of poly (*N*,*N*-diethylacrylamide). NNDEA is polymerized in the presence of Pluronic P-105 micelles, which results in an interpenetrating network that stabilizes the micellar core. Cross-linking the NNDEA with *N*,*N*-bis(acryloyl)cystamine (BAC) increases micellar stability, but it has been found that this stability disappears after several weeks. The degree of stability is determined using dynamic light scattering and the fluorescent probe diphenyl-1,3,5-hexatriene (DPH) [8].

Tests were conducted in order to determine whether such stabilization would affect the ability of the micelles to sequester and release doxorubicin. It has been shown that the amount of drug released and its subsequent re-encapsulation were not significantly different from the behavior observed for unstabilized micelles, but had the added bonus of slow dissolution of the micellar structure. Stabilized micelles released the doxorubicin at 70-kHz ultrasound [9].

In developing drug delivery systems using Pluronic block copolymers, knowing the critical micelle concentration (CMC) is instrumental [10], [11]. The CMC is defined as the concentration of block copolymer at which micelles are formed. Block copolymer concentrations below the CMC will not form micelles; rather, the block copolymer will exist in the form of unimers [12]. It is important to note here that when the copolymers are diluted in body fluids, the CMC is the factor that determines the stability of micelles [11]. The CMC of Pluronic P105 is approximately 1 wt% at room temperature [13].

Pluronic copolymers at different aggregation states have been tested as drug carriers [14], [4], [15]-[18]. Pluronic molecules in the unimeric form, below the critical micelle concentration, were found to greatly enhance the cytotoxic activity of a wide variety of drugs. Above the critical micellar concentration, Pluronic molecules form dense micelles with a lipophilic core that encapsulate the drugs within that core [19].

2.2 Drug Targeting

There are three types of targeting: passive, active and triggered targeting. Healthy tissue blood vessels have tight inter-endothelial junctions, while tumors exhibit defective microvasculature with large inter-endothelial gaps. Those gaps result in heightened vascular permeability. Passive targeting is based on the enhanced permeability and retention (EPR) effect that allows extravasation of drug-loaded nanoparticles through such defective microvasculature in the tumor. Furthermore, tumors express poor lymphatic drainage which serves to ensure that the extravasated particles are retained for longer times in the tumor tissue. Extravasation of nanoparticles would not be possible in healthy tissue blood vessels. The EPR effect that would allow for the accumulation of nanoparticles in the tumor tissue requires sufficient residence time for the particle in circulation. Coating nanoparticles with poly(ethylene-oxide) chains allows for an increase in carrier circulation in the body since the coating suppresses blood-protein adsorption and the recognition of the particle by cells of the retico-endothelial system (RES) [20]. Therefore, problems with colloidal drug delivery systems include short blood half-lives and nonspecific targeting. Carrier molecules are rapidly eliminated from the blood due to the recognition by the macrophages of the mononuclear phagocyte system (MPS) as a consequence of the adsorption of blood proteins onto the surface of the carriers. This causes the accumulation of carrier in the MPS organs, such as the liver and the spleen. For this purpose PEG is used in the modification of carrier surface. To solve the problem of site-specific targeting, small nonantigenic ligands such as folic acid can be used [21].

Site specific targeting is possible because a wide variety of human tumors, especially ovarian carcinoma, have shown vast overexpression of folate binding protein, a glycosylphosphatidylinositol-anchored cell surface receptor for the vitamin folic acid [22]. Experiments with folate-targeted Dox have shown that cells that overexpress the folate receptor, such as KB and HeLa cells, demonstrate significant uptake of the drug. Cells such as W1-38 fibroblasts take up less drug since they do not over-express the folate receptor [23]. Studies have also shown that the number of folic acid targeting ligands needs to be optimized in order to maximize Dox uptake [24]. Another study used nanogels with attached folate-targeting groups as carriers of Dox and other anti-cancer drugs to target ovarian cancer. The study was conducted *in vivo* and strong anti-tumor effect has been observed [25].

To synthesize folated Pluronic P105 micelles (P105-FA), 1,1-carbonyldiimidazole (CDI, Sigma Aldrich) is used. Approximately 1.026 gm of folic acid (Sigma Aldrich) is dissolved in 100 ml of dried DMSO followed by adding 0.414 gm CDI and is allowed to react for 4 hours under dark conditions at room temperature. After activating the folic acid, 30.2 grams of Pluronic P105 (BASF), dried overnight under vacuum, is added to the above solution. The activated CDI and Pluronic P105 are allowed to react for 20 hours at room temperature in darkness. At the conclusion of the reaction, the product is dialyzed (Spectra Millipore MWCO 3500) against DMSO for 2 days and then against DD-water for 2 days. The purified product is then lyophilized. The formation of P105-FA is confirmed using NMR. NMR peaks calculate a yield of around 48 %. The product is then kept under -20 ^{o}C until future use [26].

2.3 Triggered Targeting

Ideally, the liposome drug delivery procedure would occur as follows: first, the liposomes loaded with the drug would be introduced and circulate with the blood. Then, a stimulus would be provided to release the drug at a controlled rate. Different types of stimuli have been tested, including pH, temperature, electric fields, and ultrasound.

Ultrasound has been found to be a viable option due to its ability to propagate into deep tissue and the fact that it can be specifically focused on the target tumor [4].

In controlled drug delivery, the release of Dox from Pluronic P105 micelles is triggered using ultrasound. Ultrasound releases the drug from micelles and enhances intracellular uptake of both released and encapsulated drug [27]. The advantages of ultrasound are that it is non-invasive, penetrates deep into the body, has a synergistic effect of the activity of drugs, and enhances transport of drugs through various membranes and tissues. Furthermore, ultrasound intensity and activity can be carefully controlled and focused, and it induces hyperthermia, which helps with further destruction of cancer cells. A study has shown that a combination of doxorubicin, ultrasound, and Pluronic P105 causes the greatest amount of damage to cancer cell DNA compare to other controls [28].

Ultrasound technology generally includes low frequency ultrasound and high frequency (diagnostic) ultrasound. Both types have their advantages and their disadvantages. The ultrasound with the longer wavelength in low frequency ultrasound is frequently difficult to focus and the resulting ultrasonic cavitation can destroy tissues within the body. High frequency ultrasound has the advantage of being easily focused; however, cavitation is weak, which reduces effect on drug release [29].

A solution of diblock copolymer micelles exposed to high intensity focused ultrasound has been found to exhibit a decrease in pH. Tests conducted on samples revealed the cause of this to be the formation of carboxylic acid dimmers and hydroxyl groups. The results suggested that the ultrasound induced the hydrolysis reaction of some organic groups. Those results could be used to develop ultrasound-sensitive block copolymer micelles that have labile chemical bonds in the polymer structure. These bonds would then be disrupted by high intensity focused ultrasound [30].

Ultrasound triggered drug release from Pluronic P-105 micelles under pulsed ultrasound was measured using an ultrasonic exposure chamber with fluorescence detection. The frequency range studied was 20 to 90 kHz, and the concept behind the

measurements was the decrease in the intensity of the fluorescence of the drug when it was transferred from the hydrophobic core of the micelle to the aqueous environment. For the purpose of the study, two intrinsically fluorescent drugs were used – Dox and Ruboxyl. The most efficient frequency was found to be 20-kHz ultrasound, and the drug release was found to decrease at higher frequencies, despite much higher power densities. This unexpected results hint that the role of transient cavitation in drug release is significant. The study also found that drug release is higher at lower pluronic concentrations and lower if the drug is inserted deeper into the core of the micelle. Finally, the study also confirmed the re-encapsulation of the drug within the micelle between pulses of ultrasound, which prevents the harmful effect of the drug on healthy tissues [14].

The effect of ultrasonication at high frequencies on the release of Dox from Pluronic micelles and the uptake of Dox by the cancer cells was studied for promyelocytic leukemia HL-60 cells, ovarian carcinoma drug-sensitive and multi-drug resistant cells, and breast cancer MCF-7 cells. Radial trapping was used to record the cavitation events brought about by the high-frequency US. Even short exposure to high frequency ultrasound was found to greatly increase the rate of cellar uptake of Dox [31].

The kinetics of release and re-encapsulation of Dox from Pluronic P-105 micelles were then studied using a fluorescence detection exposure chamber. At a power density of 58 mW/cm^2 and a frequency of 20 kHz, experimental results showed that no significant release of Dox occurred from exposure to ultrasound for less than 0.1 s. This was the threshold value, above which the amount of release was proportionate to the pulse length. Furthermore, it was found that re-encapsulation requires at least 0.1 s of no ultrasound. The entire process of release and re-encapsulation requires around 0.6 s. A mathematical model for the release and re-encapsulation of the drug was then obtained. After fitting the data according to several mechanistic models, it has been found that the model of zero-order release with first-order re-encapsulation best fit the experimental data [32].

Further investigation into the kinetics of Dox release from Pluronic P-105 micelles was conducted and new mechanisms proposed. The first mechanism is micelle destruction, which causes the release of Dox during insonation. The micelles are destroyed because the collapsing nuclei produce cavitation effects – they may be viewed as bubbles in the insonated solution. The second mechanism, the destruction of cavitating nuclei, results in a small amount of Dox re-encapsulated which initiates a slow and partial recovery phase, reassembly of micelles, and the re-encapsulation of Dox. The third mechanism is the reassembly of micelles and the fourth mechanism is the re-encapsulation of Dox. Both mechanisms do not show a dependence on ultrasound and they are responsible for maintaining drug release at a partial level. Micellar size was described using a normal distribution [33].

Experiments have also shown that ultrasound disturbs the covalent network of the stabilized micelles, but the time constant of the degradation of the network is much greater than the time constant related to drug release from micelles. The results were used to deduce degradation kinetics of stabilized Pluronic P-105 micelles [34]. It was also shown that a synergism exists between Dox and ultrasound [35].

Studies have also shown that the rate constant of Dox release depends on the degree of stabilization (cross-linking), but the re-encapsulation rate constant is roughly the same for stabilized and unstabilized micelles [36]. Previous publications have shown that low frequency (70 kHz) US releases around 2% of Dox in 2 seconds from the core of stabilized Pluronic P105 micelles, when a cross-linked network of N,N-diethylacrylamide is used as a stabilizing agent. A study was conducted to study the degradation kinetics of stabilized Pluronic micelles in the 24 hours following exposure to US that lasted 2 hours. The experiments showed that US disrupts the covalent network of the stabilized micelles, but the time constant for degradation is very long compared to the time constant of drug release from the micelles. Studies were conducted using US frequencies of 70 and 476 kHz and degradation rates were found to be approximately the same for both frequencies [37].

Later investigations into the thermodynamic characteristics of US activated release of Dox from micelles allowed for calculating the thermodynamic activation energy for micelle re-assembly and residual activation energies for micelle destruction. The model found that residual activation energy decreased as the acoustic intensity increased. Furthermore, higher temperatures were found to encourage micelle destruction but hindered the re-assembly of micelles [38], [39].

The dynamic release of Dox from Pluronic P-105 micelles has been modeled using an artificial neural network (ANN). It was used to model the release of Dox at two frequencies and under different ultrasonic power intensities. A controller was then designed which adjusts the ultrasound frequency, intensity, and pulse length in order to ensure a constant rate of Dox release. This controller has been successfully tested [40]. Moreover, some ANN control algorithms have been implemented in model predictive control (MPC) [41], [42].

Artificial neural networks, as a nonlinear modeling technique, are able to capture and estimate the behavior a certain system exhibits when exposed to various operating conditions. Sensitivity analysis using ANN has shown that lower frequencies contribute to the most efficient Doxorubicin release, and the release increases with power density. The latter finding strongly suggests that cavitation plays a role in US triggered drug release. Also, drug release is not a strong function of temperature, and lower copolymer concentrations contribute to a higher rate of drug release [43]. NN-MPC has been shows to effectively model, control, and optimize Dox release from Pluronic P-105 micelles, with the feed-forward NN accurately capturing the data of dynamic Dox release [3].

2.4 In Vitro

The effectiveness of ultrasound-triggered drug release from micelles was tested by exposing HL-60 cells to free Dox and Dox encapsulated in Pluronic micelles. Cells exposed to encapsulated Dox survived much longer than the cells exposed to free Dox. However, with the application of 70-kHz ultrasound, cells exposed to encapsulated Dox

were destroyed much sooner than cells exposed to free Dox. These results suggest that micelles sequester the drug from the cells, hence increasing their survival, and ultrasound releases the drug from the carrier [1].

In order to measure the uptake of Dox by HL-60 cells, 70-kHz ultrasound was pulsed It was found that with constant spaces of time between bursts and with a constant total insonation time, the amount of uptake of Dox by the cells increased as the length of insonation increased (up to 3.0 sec). The time between bursts had no effect on the amount of uptake of the drug [44]. This indicates that the cells did not permit the return of any Dox back to the micelles, other than the amount that could have diffused back into the micelles during the period between bursts. The total calculated time to reach 90% of complete uptake was 2.5 seconds of US [1].

The effect of ultrasound on the cytotoxicity of cytosine arabinoside to HL-60 cells was tested and an increase in cell death was observed. It was concluded that insonation disturbed and modified the cell membrane, thus increasing the amount of drug taken in by the cell [45].

Another study later showed that the perturbation in the cell membrane was due to the pores that ultrasound formed – a phenomenon termed sonoporation. In this particular publication, sonoporation caused the cytoplasm of HL-60 cells to leak out of those pores [46].

2.5 In Vivo

The most convenient model for *in vivo* experiments uses rats and mice injected with a specific tumor; however, hamsters and rabbits are also used for *in vivo* experiments. There is a synergistic effect between chemotherapy drugs and ultrasound. A study has shown that exposure to ultrasound that lasted one hour made Dox significantly more toxic to Chinese hamster lung cancer [47].

A tumor-bearing rat model was used to investigate the effect of ultrasound on tumor growth rate and to determine which frequency works best in the treatment. It was found that the combination of drug and ultrasound resulted in a slower tumor growth rate than drug delivered alone. It was also found that ultrasound frequency does not affect the growth rate, as 20- and 476-kHz treatments yielded the same results [1].

Another *in vivo* study was conducted using 42 rats, which were inoculated in each hind leg with a colon carcinogen DHD/K12/TRb tumor cell line. Six weeks after the tumor injections, Dox, encapsulated in stabilized Pluronic micelles, was administered weekly with an IV injection [48]. The study showed that Dox concentrations of 8 mg/kg were lethal within two weeks, while 5.33 and 4.0 mg/kg were lethal within six weeks. Concentrations of 1.33 and 2.67 mg/kg did not produce death. The general results looked promising, as the tumors that were exposed to a combination of encapsulated Dox and ultrasound did not grow as much as the tumors not exposed to ultrasound. The tumor treated with ultrasound actually slowed in growth. A later study reported the distribution of Dox in rats undergoing ultrasound-mediated drug delivery [49].

A study using a mouse model showed that tumors exposed to ultrasound accumulated a significantly greater amount of micelles than non-insonated tumors [50]. The same study also showed that the cardiotoxicity of Dox is reduced by the use of micelles as the encapsulated Dox did not accumulate in the heart of the mice.

It is important to examine the mechanism by which micelles deliver anti-cancer drugs. One of the pathways that micelles are taken up by cancer cells is endocytosis, a mechanism by which a cell internalizes macromolecules from the surrounding tissue fluid. Two types of endocytosis exist: pinocytosis and receptor-mediated endocytosis. Pinocytosis is characterized by the uptake of small droplets of extracellular fluid, and any material dissolved in it, by endocytic vesicles. Receptor-mediated endocytosis, as the name suggests, utilizes a specific receptor on the cell membrane surface. This receptor binds to the target molecule, or ligand, which in turn sends a signal to the cell membrane to fold in on itself, forming a small vesicle through which the molecule is internalized [51].

Investigation into the mechanisms of the uptake of the micelles by cancer cells was conducted in an attempt to explain the shielding effect Pluronic micelles have on the drug. Below the critical micelle concentration (CMC), the uptake of Pluronic micelles was proportional to the concentration of the incubation medium. Above the CMC, intracellular uptake of the micelles was far less efficient. The data led to the belief that Pluronic micelles are internalized through fluid-phase endocytosis, rather than diffusion through plasma membranes. The experiments were conducted using flow cytometry, fluorescence spectroscopy, and confocal and fluorescence microscopy. Pluronic P-105 was fluorescently labeled. Human Leukemia (HL-60) cells were used in these experiments [52].

It was later found that the increase in the accumulation of doxorubicin in HL-50 cells was not due to increased endocytosis due to ultrasonication. Rather, it was suspected that sonoporation plays an important role in the process. This led to several hypotheses being proposed as to how ultrasound increases the rate of uptake of the drug by the cells.

One hypothesis states that acoustic streaming, or momentum transfer from sound waves to biological fluid, and microconvection created by oscillating bubbles of gas in the liquid are responsible for the disruption of the cell membrane. The perturbed cell membrane is rendered more permeable to the drug. Acoustic pressure ranges from high to low, which causes the oscillating bubbles of gas to grow in size and then shrink, creating shear flow around themselves. If the bubbles do not exhibit complete collapse during their shrinkage cycle, then stable cavitation occurs. When the bubble collapses, collapse cavitation (also termed transient cavitation) results. Both forms of cavitation create high shear stresses, which create holes in the cell membrane [53]. Experiments have shown, however, that increasing the static pressure represses bubble cavitation [54]. There is a strong correlation between the amount of drug release and subharmonic acoustic emissions, which is attributed to collapse cavitation that disturbs the micelle structure and results in the release of the drug [55].

Another hypothesis claims that exposure to ultrasound increases the concentration of the drug (due to its release from micelles), but does not alter the permeability of the

cell membrane. The high concentration outside the cell membrane creates a sufficiently high diffusion gradient for drug uptake by the cells. However, this hypothesis was readily dismissed when several studies demonstrated that ultrasound does indeed increase the permeability of the cell membrane [53]. The third hypothesis states that ultrasound increases the rate of endocytosis. Tests have revealed that while ultrasound enhances drug uptake, it doesnot do soby increasing the rate of endocytosis [53].

Thus, acoustically activated micellar drug delivery systems are rendered effective due to two main mechanisms. Ultrasound results in drug release since it disrupts the core of polymeric micelles. In addition, ultrasound has been shown to form micropores in the membranes of cancer cells – a phenomenon called sonoporation, which allows drugs to passively diffuse into the cells [2].

The comet assay is used to quantify DNA damage by measuring the length and the fraction of broken DNA strands. A large amount of DNA damage indicates the death of the cell. An experiment was conducted in which cells were treated with various combinations of Dox US, and Pluronic P105. The cells were sonicated and lysed, then placed in an electrophoresis buffer, which resulted in further DNA unwinding, after which electrophoresis was performed. Electrophoresis displayed the migration of intrinsically negative DNA away from the negative electrode and towards the positive electrode. Then a distilled water bath was used to reanneal the DNA, which was then stained with propidium iodide, a fluorescent dye. Upon analysis, the electrophoresed DNA looks like a comet, with the damaged DNA migration pattern forming the tail, and undamaged DNA forming the head. The parameters obtained are total DNA, the percentage of DNA in the head and the tail of the comet, the tail length, and the tail moment. The tail moment is the best parameter for the determination of DNA damage since it takes into account both the length of the tail and the fraction of DNA contained within the tail [56].

Ultrasound alone was found to cause no damage to DNA, whether with or without P105. Dox contained in P105 caused no damage unless US was applied, and free Dox and Dox with ultrasound display various degrees of damage. DNA damage was most

pronounced when a combination of Dox, P105, and US was applied [56]. In conclusion, Dox is trapped within P105, unless US is used to trigger its release, and US speeds up the extent of damage causes by Dox, and works even better when Dox is in P105.

Chapter 3: Objectives

The objectives of this thesis are as follows:

1. To calculate the percent release of Dox from folated and non-folated micelles at different power densities from fluorescence intensity data.
2. To test how well two mathematical models fit release and re-encapsulation dynamic experimental data.
3. To calculate release and re-encapsulation rate constants for targeted and non-targeted micelles as a function of power density. The acoustic activation power density and Gibbs free energy can then be calculated for the release and re-encapsulation processes.
4. To use artificial neural network (ANN) to predict release.

Chapter 4: Data Analysis

4.1 Measuring Release from Targeted and Non-Targeted Micelles

Dox is intrinsically fluorescent, but when it is released from micelles when the ultrasound is switched on, its fluorescence is quenched by the surrounding aqueous environment. Hence, in Fig.2, a sudden drop in fluorescence intensity is observed at around 9 seconds. When re-encapsulation begins at around 19 seconds, Dox regains its fluorescence when its exposure to the aqueous environment is hindered by the micellar structure. For each power density, the data was subdivided into runs, with each runs containing three release pluses. Fig.2 below is a representative example of one release pulse at 5.01 W/cm^2 for acoustic release of Dox from targeted micelles. The three distinct regions that make up the pulse correspond to the fluorescence intensity of Dox at the ultrasound level – the initial intensity, the intensity when the ultrasound is switched on (release of drug takes place), and the intensity when the ultrasound is switched off (re-encapsulation of drug occurs). The flat profile below the pulse corresponds to the fluorescence intensity of Dox in phosphate-buffered saline (PBS) and serves as the base-line for calculations, also called the 'free Dox fluorescence intensity'. All data were later shifted to start at time = 0. Each run was subdivided into three regions, and an average for each region was obtained.

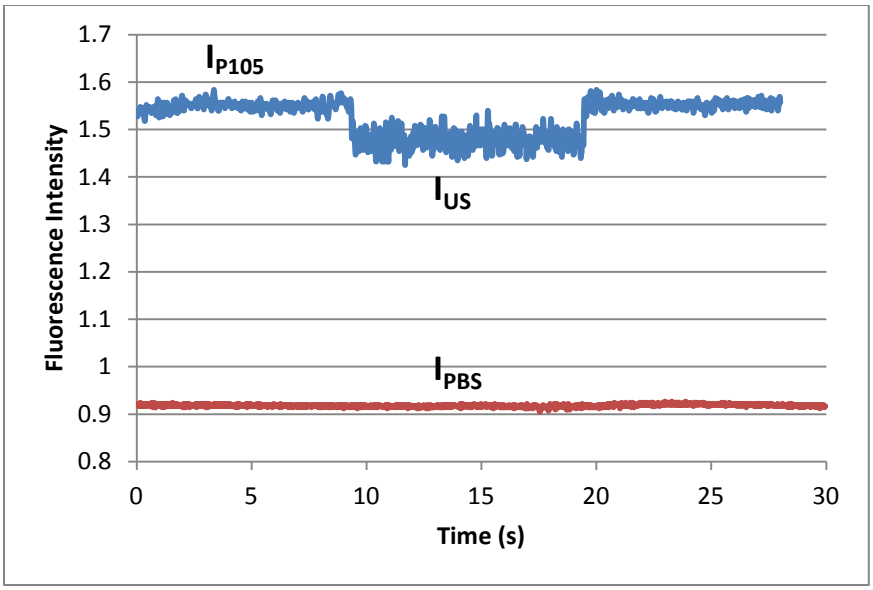

Figure 2. An example showing the raw data for one release pulse for folated micelles at 5.01 W/cm^2.

The first region average is the value used in calculating the percent release from the fluorescence intensity at each point according to the following equation:

$$\%\, release = [\frac{I_{P105} - I_{US}}{I_{P105} - I_{PBS}}] \qquad (4\text{-}1)$$

and,

$$\%\, encapsulated = 1 - [\frac{I_{P105} - I_{US}}{I_{P105} - I_{PBS}}] \qquad (4\text{-}2)$$

The average percent release for each run was obtained and all percents of release were then averaged for each run and the standard deviation calculated.

4.2 Materials and Methods

Pluronic P105 with folate attached to their surface was conjugated during Dr. Ghaleb Husseini's sabbatical at EPFL. P105-FA was synthesized using 1,1-carbonyldiimidazole (CDI, Sigma Aldrich) [57]. Approximately 1.026 g of folic acid (Sigma Aldrich) was dissolved in 100 ml of dried DMSO. Then 0.414 g CDI was added and allowed to react for 4 hours under dark conditions at room temperature. After this activation of the FA, 30.2 g of Pluronic P105 (BASF), which was dried overnight under vacuum, was added to the above solution. The activated CDI and Pluronic P105 were allowed to react for 20 hours at room temperature in darkness. At the conclusion of the reaction, the product was dialyzed (Spectra Millipore MWCO 3500) against DMSO for 2 days and then against DD-water for 2 days. The purified product was then lyophilized and stored at -20°C. The formation of P105-FA was confirmed using NMR which showed a broad peak at 3.7 ppm (attributed to PEG) and characteristic peaks attributed to folic acid at 2.3, 6.6, 7.6 and 8.6 ppm. These NMR peaks were also used to calculate a yield of 48 %. For release experiments, P105-FA (48% yield) was dissolved in DD-water to make a final concentration of 5 wt. %. Dox (Sigma Aldrich) was introduced into the micelles by mixing at room temperature. Using dynamic light scattering, the size of these micelles was measured to be 10.2 ± 2.2 nm.

To measure the release, a custom chamber was built to measure the change in fluorescence and hence the Dox release in the presence and absence of ultrasound [58]. The beam of an argon ion laser (Ion Laser Technology, Model 5500 A) was directed to a beam splitter attenuator (metal film neutral density attenuator). The intensity of the split portion of the beam was measured by a photo detector (used to monitor the laser power) and the other portion of the beam was directed into a fiber optic bundle.

The drug concentration was quantified by measuring fluorescence emissions produced by an excitation wavelength of 488 nm. A fiber optic probe (100 bundled multinode fibers, approximately 40 cm in length) was used to deliver the excitation light

to the sample and to collect fluorescence emissions. The emitted light was directed through a multinode dielectric band and filter (Omega Optical Model 535DF35) to a silicon detector (EG and G 450-1). The filter was used to cut off any emissions below 517 nm, including any Rayleigh-scattered laser light. Fluorescence measurements were digitized for computer storage and processing. To mimic physiological conditions, the temperature of the ultrasonic exposure chamber was maintained at 37 ^{o}C using a thermostated bath.

The chamber described above was used to measure the kinetics of acoustically activated drug release from micelles. Dox exhibits a large decrease in fluorescence when transferred from the hydrophobic core of the micelle to the surrounding aqueous solution. Therefore, the release can be determined by measuring the decrease in fluorescence intensity upon the application of ultrasound. In these release experiments, we used a Dox concentration of 5 μg/ml. When calculating the percent release, fluorescence data were corrected to account for Dox quenching by folic acid. Ultrasound was applied using a 70-kHz ultrasonicating bath (SC-40, Sonicor, Copiaque, NY) equipped with a single piezoceramic transducer that is driven at about 70 kHz. The best description of the waveform is that of a 70-kHz wave amplitude modulated sinusoidally at about 0.12 kHz. The bath was powered by 60-Hz AC voltage from a variable AC transformer (variac). The voltage from the variac to the sonicating bath was adjusted to produce differing intensities of continuous ultrasound and these intensities were measured using a hydrophone (Bruel and Kjaer model 8103, Decatur, GA). The ultrasound was manually turned on and off every 10 seconds.

4.2.1 Acoustic Measurements

Ultrasonic power density measurements were obtained using a calibrated hydrophone (Bruel and Kjaer model 8103, Decatur, GA) whose response was measured with an oscilloscope. After measurements of Dox fluorescence, the fiber optic was replaced with the hydrophone in the same location, and the hydrophone response was

recorded at the same settings as used for the fluorescence measurements. The average acoustic intensity was calculated from $I=V_{rms}^2 Q^2/Z$ where Q is the calibration factor, Z is the acoustic impedance (1.5 $x10^6$ kg/m^2 s), and V_{rms} is the root-mean-squared voltage of the hydrophone signal.

The derivation of the equation used was as follows:

Acoustic pressure is changed to voltage. From the voltage, we can calculate the power density:

$$dB = 10 \log(I/I_{ref}) \quad (4\text{-}3)$$

$$dB = 20 \log(V/V_{ref}) \quad (4\text{-}4)$$

$$dB = 20 \log(P/P_{ref}) \quad (4\text{-}5)$$

The basic definition of $dB = 20 \log_{10} (X/IV/\mu Pa)$ (4-6)

It is the log ratio of signals.

For Hydrophone #1, voltage sensitivity gives -211.8 dB.

$(-211.8/20)\ dB = -10.59 = \log_{10} (X/IV/\mu Pa)$

$X/IV/\mu Pa = 10^{-10.59} = 2.5704 \times 10^{-11}$ V/µPa

2.5704×10^{-11} (V/µPa) x 10^6 (µPa/1 Pa) x 10^6 (mV/1 V) = 25.704 mV/Pa = 25.704×10^{-6} V/Pa

$$\bar{I} = \frac{\bar{P}}{z} = \left(\frac{\sqrt{\overline{P^2}}}{z}\right)^2 = \frac{\left(\sqrt{V^2\left(\frac{Pa}{25.704\times10^{-6}\,V}\right)}\right)^2}{z^2} \quad (4\text{-}7)$$

$$z_{H2O} = 1.5 \times 10^6 \ \frac{kg}{m^2 s} \quad (4\text{-}8)$$

$$V_{rms} = \sqrt{\overline{V^2}} \quad (4\text{-}9)$$

$$\bar{I} = \frac{Pa^2}{\frac{(25.704\times10^{-6})^2}{1.5\times10^6 \frac{kg}{m^2 s}}} \quad (4\text{-}10)$$

$$V_{rms} = \frac{1}{9.91\times10^{-4}} = \frac{1010\frac{W}{m^2}V_{rms}^2}{V^2} \quad (4\text{-}11)$$

$$\bar{I} = \frac{1010\frac{W}{m^2}V_{rms}^2}{V^2} \times \left(\frac{1\ m}{100\ cm}\right)^2 = 0.101\ \frac{W/cm^2}{V^2}V_{rms}^2 \quad (4\text{-}12)$$

Efficiency at 70 kHz = -3.2 dB

Correction at 70 kHz = $10^{\frac{-3.2\ dB}{10\ dB}}$ = 0.479

At 70 kHz:

$$\bar{I} = 1010\frac{W}{cm^2} \times \frac{1}{0.479} = \frac{2.11\times10^{-1}}{V^2}\ V_{rms}^2\ [\frac{W}{cm^2}] \quad (4\text{-}13)$$

4.3 Results and Discussion

4.3.1 Comparison of release from folated and non-folated micelles

The amount of Dox release as a function of ultrasound intensity was measured at a frequency of 70 kHz and the results were evaluated. Dox fluorescence is drastically higher inside the core of the micelles as compared to its quenched fluorescence upon exposure to an aqueous environment.

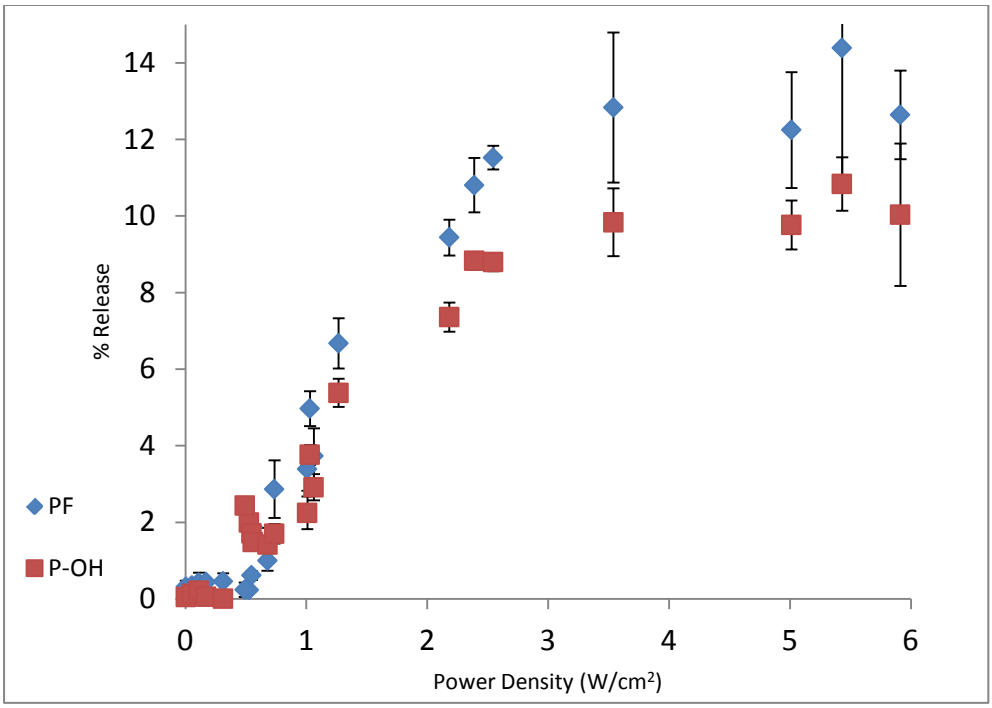

Figure 3. Percent release of Dox from targeted and un-targeted micelels as a function of acoustic power density at 70 kHz.

Fig.3 summarizes the percent of drug release from folated and untargeted micelles as a function of acoustic power density at 70 kHz. The plot can be subdivided into three distinct regions which are followed by both folated and untargeted micelles. At low power densities, the measured drug release is very small and cannot be distinguished from the release in conditions of no ultrasound. This trend continues up till about 0.5 W/cm^2, after which the release from folated micelles follows an almost linear increase with the power densities up until about 3 W/cm^2 and which constitutes the second region on the plot. Meanwhile, the release from non-targeted micelles is a little less linear, with some erratic behavior observed around 0.5 W/cm^2. After that power density, however, the release from untargeted micelles is always lower than the release from the folated micelles. In the third region, above 3 W/cm^2, both types of micelles demonstrate a fairly constant amount of release. For folated micelles, this amounts to approximately 13%, while for the untargeted micelles it is only about 10%.

Thus, the data shows the existence of two thresholds, 0.5 W/cm^2 and 3 W/cm^2, which implicate the role of inertial cavitation in the drug release. The lower threshold value is believed to signify inertial cavitation in water, but while there is no explanation for the upper threshold, it has been reported in other studies [59], [60]. At the lower threshold, a possible explanation is that transient cavitation produces shock waves that rupture the micelles, resulting in the release of the encapsulated drug into the aqueous environment. It can be hypothesized that the higher release from folated micelles can be attributed to the compromised integrity of the micelle structure due to the attached folic acid.

An ultrasonic field is an oscillating pressure field that causes the gas bubbles present in the aqueous environment to expand and contract in a similarly oscillatory matter. This oscillation cause high shear stress close to the surface of the gas bubble. These stresses decrease as the distance from the cavitating bubble increases. It is believed that such high shear stress is what causes the rupture of micelles floating near the cavitating gas bubbles in the aqueous environment. This results in the release of Dox which may be taken up by cells surrounding the ruptured micelle or which may diffuse back into other micelles nearby. Re-encapsulation of Dox occurs when ultrasound is turned off and micelles re-assemble as the Dox diffuses into the newly-formed micelles.

4.3.2 Testing statistical significance

The non-parametric Mann-Whitney U test was conducted on the folated and nontargeted micelle release data for each power density in order to assess the statistical significance of experimental data. The test would serve to determine whether the greater observed release from folated micelles was indeed statistically significant or merely the result of coincidence. The Mann-Whitney test was chosen because the data was from two unpaired groups and did not follow a Gaussian distribution. If the significance level is lower than 5% (0.05), then the results could not have occurred by coincidence. The lower power densities did not have enough data points to give accurate results, but power densities of 1.03 W/cm^2 and higher all gave significance levels of lower than 5%.

Therefore, it was confirmed that Dox release from targeted micelles is indeed higher than its release from non-targeted carriers. The results of the test are reported in Table 4.1, with 'N' representing the sample size.

Table 1. Results of the Mann-Whitney U Test

Power Density (W/cm^2)	Median PF	Median P105	N PF	N P105	Significance Level
0.00	0.0038	0.0001	3	3	0.0809
0.06	0.0037	0.0000	3	3	0.3758
0.11	0.0028	0.0025	3	3	0.3827
0.17	0.0041	0.0000	3	3	0.0765
0.31	0.0045	0.0000	3	3	0.0765
0.53	0.0021	0.0208	3	3	0.0809
0.49	0.0018	0.0243	3	3	0.0809
0.55	0.0066	0.0177	3	3	0.0809
0.56	0.0181	0.0148	3	3	0.0809
0.68	0.0105	0.0163	3	3	0.3827
0.74	0.0323	0.0184	3	3	0.0809
1.01	0.0306	0.0228	3	3	0.0809
1.03	0.0494	0.0382	9	6	0.0018
1.27	0.0677	0.0528	9	6	0.008
2.18	0.0946	0.0738	9	6	0.0018
2.39	0.1076	0.0894	9	6	0.0018
2.55	0.1165	0.0884	6	6	0.005
3.54	0.1285	0.1011	6	6	0.0306
5.01	0.1210	0.0986	9	6	0.008
5.43	0.1300	0.1085	15	6	0.0035
5.91	0.1242	0.1041	12	6	0.0032

Chapter 5: Mathematical Modeling

5.1 Model 1: first-order release and first-order re-encapsulation

The data were fitted using two mathematical models in order to obtain the rate constants for release and re-encapsulation of the Dox from folate targeted micelles and non-targeted micelles under the action of ultrasound. The first model assumes first-order release and first-order re-encapsulation, while the second model assumes zero-order release and first-order re-encapsulation. Thus, the equations, and hence the rate constants, for re-encapsulation are common to both models. The first model assumes that the rate of release of Dox is first order with respect to the amount of encapsulated Dox, and that the rate of re-encapsulation is first order with respect to free Dox in solution. Physically, it is hypothesized that ultrasound does not destroy the micelles, thus keeping their number constant, but only perturbs them enough to allow the drug to partially leak out. It is assumed, simultaneously, that Dox is re-encapsulated back into the micelles at a rate proportional to the amount of free drug in solution and the micelle concentration [3].

The release and re-encapsulation are modeled as two first-order competing events that occur simultaneously. The differential equation that describes the release is as follows:

$$\left.\frac{\mathrm{dE}}{\mathrm{dt}}\right|_{\mathrm{US}} = -\mathrm{k_{r1}} + \mathrm{k_e}\,\mathrm{F} = -\mathrm{k_{r1}} + \mathrm{k_e}\,(\mathrm{T} - \mathrm{E}) = -(\mathrm{k_{r1}} + \mathrm{k_e})\mathrm{E} + \mathrm{k_e}\,\mathrm{T} \tag{5-1}$$

To solve Eq. (5-1), the integrating factor method can be used.

Rearranging,

$$\frac{\mathrm{dE}}{\mathrm{dt}} + (\mathrm{k_{r1}} + \mathrm{k_e})\mathrm{E} = \mathrm{k_e}\,\mathrm{T} \tag{5-2}$$

The integrating factor is $e^{\int(\mathrm{k_{r1}}+\mathrm{k_e})dt} = e^{(\mathrm{k_{r1}}+\mathrm{k_e})t}$. (5-3)

Multiplying both sides of Eq. (5-2) by the integrating factor gives:

$$e^{(\mathrm{k_{r1}}+\mathrm{k_e})t}\frac{\mathrm{dE}}{\mathrm{dt}} + (\mathrm{k_{r1}} + \mathrm{k_e})e^{(\mathrm{k_{r1}}+\mathrm{k_e})t}\mathrm{E} = (\mathrm{k_e}\,\mathrm{T})e^{(\mathrm{k_{r1}}+\mathrm{k_e})t} \tag{5-4}$$

The left hand side of Eq. (5-4) follows the product rule, so the equation can be rewritten as such:

$$\frac{d}{dt}\left(\mathrm{E}e^{(\mathrm{k_{r1}}+\mathrm{k_e})t}\right) = (\mathrm{k_e\,T})e^{(\mathrm{k_{r1}}+\mathrm{k_e})t} \tag{5-5}$$

Integrating both sides of Eq. (5-5):

$$\int \frac{d}{dt}\left(\mathrm{E}e^{(\mathrm{k_{r1}}+\mathrm{k_e})t}\right) dt = \int (\mathrm{k_e\,T})e^{(\mathrm{k_{r1}}+\mathrm{k_e})t}\, dt \tag{5-6}$$

$$\mathrm{E}e^{(\mathrm{k_{r1}}+\mathrm{k_e})t} + C_1 = (\mathrm{k_e\,T})\frac{1}{(\mathrm{k_{r1}}+\mathrm{k_e})}e^{(\mathrm{k_{r1}}+\mathrm{k_e})t} + C_2 \tag{5-7}$$

Let $C_1 - C_2 = C$

Eq. (5-7) becomes:

$$\mathrm{E}e^{(\mathrm{k_{r1}}+\mathrm{k_e})t} + C = (\mathrm{k_e\,T})\frac{1}{(\mathrm{k_{r1}}+\mathrm{k_e})}e^{(\mathrm{k_{r1}}+\mathrm{k_e})t} \tag{5-8}$$

The initial condition used to find C is that at t=0, E=T. Thus,

$$T + C = \left(T\frac{k_e}{(\mathrm{k_{r1}}+\mathrm{k_e})}\right) \Rightarrow C = \frac{k_e T}{(\mathrm{k_{r1}}+\mathrm{k_e})} - T \tag{5-9}$$

Substituting for C,

$$\mathrm{E}e^{(\mathrm{k_{r1}}+\mathrm{k_e})t} + \frac{k_e T}{(\mathrm{k_{r1}}+\mathrm{k_e})} - T = \left(T\frac{k_e}{(\mathrm{k_{r1}}+\mathrm{k_e})}\right)e^{(\mathrm{k_{r1}}+\mathrm{k_e})t} \tag{5-10}$$

Rearranging,

$$E = [\left(T\frac{k_e}{(\mathrm{k_{r1}}+\mathrm{k_e})}\right)e^{(\mathrm{k_{r1}}+\mathrm{k_e})t} - \frac{k_e T}{(\mathrm{k_{r1}}+\mathrm{k_e})} + T]e^{-(\mathrm{k_{r1}}+\mathrm{k_e})t} \tag{5-11}$$

So the solution after dividing through by T is:

$$\left.\frac{\mathrm{E(t)}}{\mathrm{T}}\right|_{\mathrm{US}} = \left(1 - \frac{k_e}{(\mathrm{k_{r1}}+\mathrm{k_e})}\right)e^{-(\mathrm{k_{r1}}+\mathrm{k_e})t} + \frac{k_e}{(\mathrm{k_{r1}}+\mathrm{k_e})} \tag{5-12}$$

When the ultrasound is turned off, release is terminated and re-encapsulation of the drug

begins. The drug returns to the micelles at a rate proportional to the concentration of free drug. During the period of re-encapsulation, the following equation describes the rate of change in the encapsulated Dox:

$$\left.\frac{dE}{dT}\right|_{no\ US} = k_e\, F = k_e\,(T - E) \tag{5-13}$$

In Eq. (5-13), E is the concentration of encapsulated Dox, F is the concentration of free drug, k_e is the re-encapsulation first-order rate constant that is common for both models, and T is the total amount of Dox in the system. The subscript 'no US' means no ultrasound is applied. Evidently, the total amount of Dox in the system is the sum of the free and encapsulated Dox concentrations. Eq. (5-13) is a separable, first-order, ordinary differential equation that can be solved accordingly.

$$\int \frac{dE}{T-E} = \int ke\ dt \tag{5-14}$$

The initial condition (at t = 0) used to solve this equation is that E, the encapsulated Dox concentration, is the value of E at the moment when the ultrasound is turned off, $E(t_{off})$.

So at t = 0, $E = E(t_{off})$

Thus, integration yields:

$$-ln|T - E| + C_3 = k_e t + C_4 \tag{5-15}$$

Let $C_3 - C_4 = C$

Eq. (5-15) becomes:

$$-ln|T - E| + C = k_e t \tag{5-16}$$

Using the initial condition to solve for C yields:

$$C = ln\left|T - E(t_{off})\right| \tag{5-17}$$

Substituting the expression for C in Eq. (5-16) gives:

$$-ln|T - E| + ln\left|T - E(t_{off})\right| = k_e t \tag{5-18}$$

$$\ln\left(\frac{|T-E(t_{off})|}{|T-E|}\right) = k_e t \tag{5-19}$$

$$\frac{T-E(t_{off})}{T-E} = e^{k_e t} \tag{5-20}$$

Rearrange to obtain an expression for E:

$$T - E = \frac{T-E(t_{off})}{e^{k_e t}} = (T - E(t_{off}))e^{-k_e t} \tag{5-21}$$

Dividing both sides by T gives:

$$1 - \frac{E}{T} = (1 - \frac{E(t_{off})}{T})e^{-k_e t} \tag{5-22}$$

Hence, the solution is:

$$\left.\frac{E(t)}{T}\right|_{no\ US} = \left(\frac{E(t_{off})}{T} - 1\right) e^{-k_e t} + 1 \tag{5-23}$$

5.2 Model 2: zero-order release and first-order re-encapsulation

The second model proposes that Dox is released from micelles at a constant rate while the ultrasound is on, and the simultaneous rate of re-encapsulation is first-order with respect to the concentration of the free drug. This model is based on the theory that ultrasound may create transient cavitation events that result in the destruction of micelles at a constant rate, and that this rate does not depend on the micelle concentration. The destroyed micelles release the drug, but its molecules are taken up by the micelles that remained at a rate proportional to the free drug concentration. The drug can either be re-encapsulated into micelles that were not destroyed or into newly-formed ones [3].

Mathematically, the model can be represented using the equation:

$$\left.\frac{\mathrm{dE}}{\mathrm{dt}}\right|_{\mathrm{US}} = -\mathrm{k_{r2}} + \mathrm{k_e}\,\mathrm{F} = -\mathrm{k_{r2}} + \mathrm{k_e}\,(\mathrm{T} - \mathrm{E}) \tag{5-24}$$

To solve Eq. (5-24), the integrating factor method can be used.

Rearranging,

$$\frac{\mathrm{dE}}{\mathrm{dt}} + \mathrm{k_e\,E} = (\mathrm{k_e\,T} - \mathrm{k_{r2}}) \tag{5-25}$$

The integrating factor is $e^{\int \mathrm{k_e}\,dt} = e^{k_e t}$. (5-26)

Multiplying both sides of Eq. (5-25) by the integrating factor gives:

$$e^{k_e t}\frac{\mathrm{dE}}{\mathrm{dt}} + \mathrm{k_e}\,e^{k_e t}\mathrm{E} = (\mathrm{k_e\,T} - \mathrm{k_{r2}})e^{k_e t} \tag{5-27}$$

The left hand side of Eq. (5-27) follows the product rule, so the equation can be rewritten as:

$$\frac{d}{dt}(\mathrm{E}e^{k_e t}) = (\mathrm{k_e\,T} - \mathrm{k_{r2}})e^{k_e t} \tag{5-28}$$

Integrating both sides of Eq. (5-28):

$$\int \frac{d}{dt}(\mathrm{E}e^{k_e t})\,dt = \int (\mathrm{k_e\,T} - \mathrm{k_{r2}})e^{k_e t}\,dt \tag{5-29}$$

$$\mathrm{E}e^{k_e t} + C_5 = (\mathrm{k_e\,T} - \mathrm{k_{r2}})\frac{1}{k_e}e^{k_e t} + C_6 \tag{5-30}$$

Let $C_5 - C_6 = C$

Eq. (5-30) becomes:

$$\mathrm{E}e^{k_e t} + C = (\mathrm{k_e\,T} - \mathrm{k_{r2}})\frac{1}{k_e}e^{k_e t} \tag{5-31}$$

The initial condition used to find C is: at t = 0, E = T. Thus,

$$T + C = \left(T - \frac{k_{r2}}{k_e}\right) \Rightarrow C = -\frac{k_{r2}}{k_e} \tag{5-32}$$

Substituting for C,

$$\mathrm{E}e^{k_e t} - \frac{k_{r2}}{k_e} = \left(T - \frac{k_{r2}}{k_e}\right)e^{k_e t} \tag{5-33}$$

Rearranging,

$$\mathrm{E}e^{k_e t} = \left(T - \frac{k_{r2}}{k_e}\right) e^{k_e t} + \frac{k_{r2}}{k_e} \tag{5-34}$$

Dividing by $e^{k_e t}$,

$$E = \left(T - \frac{k_{r2}}{k_e}\right) + \frac{k_{r2}}{k_e} e^{-k_e t} \tag{5-35}$$

So the solution is:

$$\mathrm{E(t)}|_{\mathrm{US}} = \frac{k_{r2}}{k_e} e^{-k_e t} - \frac{k_{r2}}{k_e} + T \tag{5-36}$$

As the time approaches infinity, E/T approaches the steady state drug concentration during US exposure, which gives:

$$\mathrm{E/T}|_{\mathrm{SS}} = -\frac{k_{r2}}{k_e} + T \tag{5-37}$$

5.3 Data Fitting

The raw fluorescence data are noisy, and since the pulsing of the ultrasound was done manually, the exact on/off times do not coincide for all the experiments. For each power density, several experimental runs were conducted and then the regions were divided according to where release and re-encapsulation occurred. The curves of release versus time were plotted against time and were subsequently overlapped over the horizontal and vertical axes. The release and re-encapsulation regions were overlapped independently. Sample plots showing overlapped runs for release and re-encapsulation for folated micelles at the highest power density are shown in Fig. 4. The black line is the the average of all runs.

a)

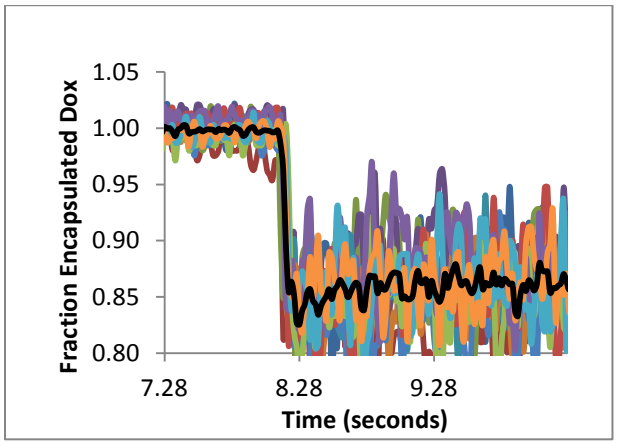

b)

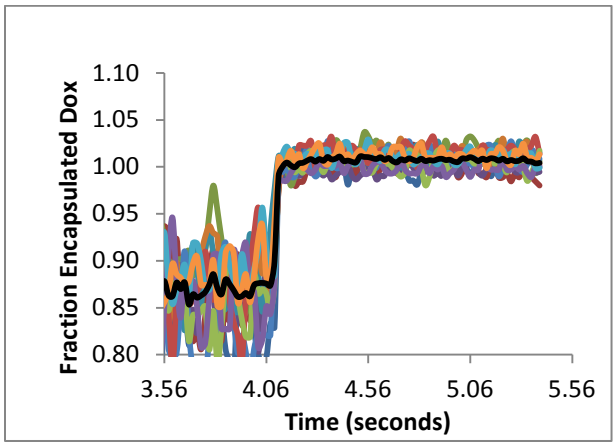

Figure 4. An example showing 12 overlayed ultrasound exposure cycles to determine the release and re-encapsulation averages when a) the ultrasound was turned on and release started, and b) when ultrasound was turned off and re-encapsulation began. Data shown are for folated micelles at 5.91 W/cm^2.

Because the data is noisy, a five-point moving average is taken instead of the regular average. Figs. 5 and 6 are inserted to show how the five-point moving average compares to the regular average for release and re-encapsulation at one particular power density. The plots show that the five-point moving average compares well to the regular average and that using the five-point average to reduce the effects of noise is a viable alternative.

a)

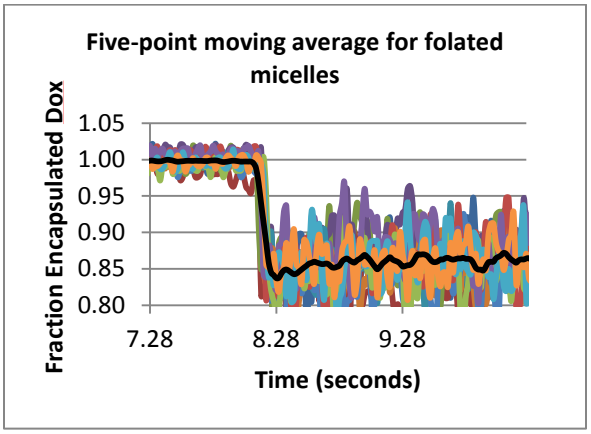

b)

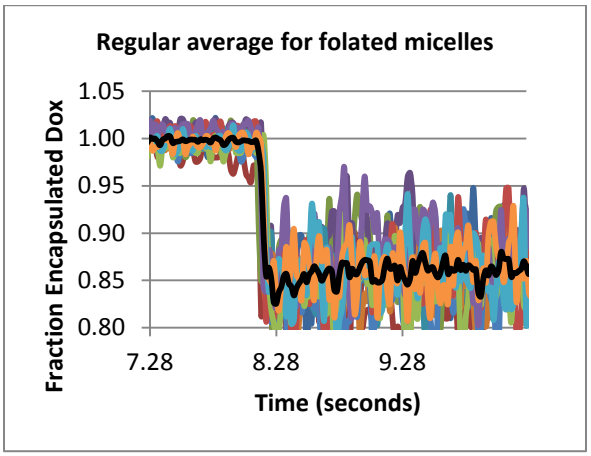

Figure 5. A comparison between the regular and five point moving averages for release from folated micelles at 5.91 W/cm^2.

a)

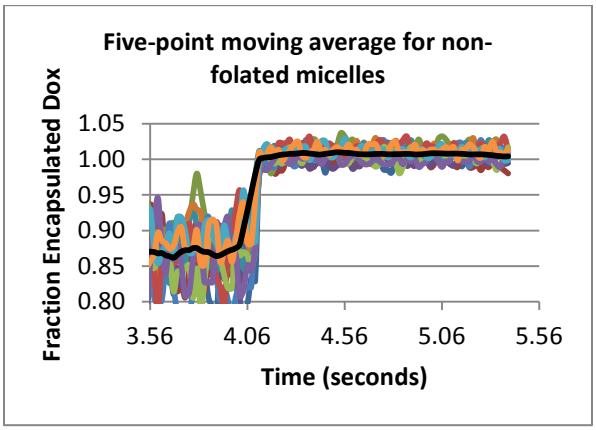

b)

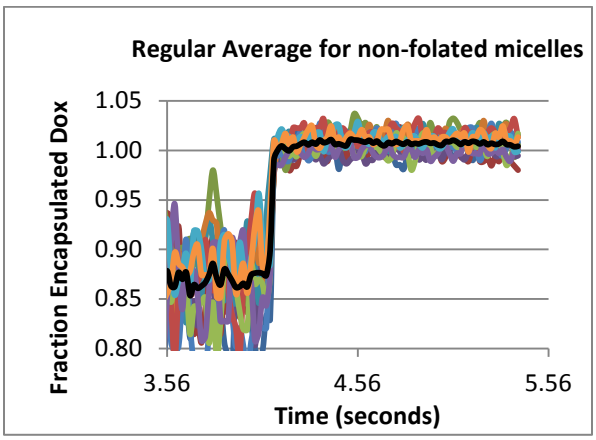

Figure 6. A comparison between the regular and five point moving averages for re-encapsulation into non-folated micelles at 5.91 W/cm^2.

The values corresponding to the entire duration of the re-encapsulation were isolated from the average and they corresponded to the E/T of the data. T was the total amount of Dox in the solution and it is equal to 4.5 µg/ml. A plot of $\ln[\frac{\frac{E}{T}-1}{\frac{E(toff)}{T}-1}]$ versus time, gave a slope giving the value for the re-encapsulation rate constant, k_e. $E(t_{off})/T$ was obtained from the plot.

As seen in the mathematical model, k_r from model 2 was then obtained as such:

$$k_r = Rk_eT \quad (5\text{-}38)$$

Where R, the release, corresponds to (1-E/T).

The release rate constant was calculated from model 2 rather than model 1 because model 1 was found to poorly fit the data. The best fit was provided by the model with zero-order release and first-order re-encapsulation. The validity of this model's fit has also been reported in other studies [43]. Fig. 7 was then generated for one power density for release and re-encapsulation from folated micelles to test how well the mathematical model fit the data. Similarly, Fig. 8 was generated for non-folated micelles. The inserts show the log transforms of the data and the model fit which were initially used to test the model.

a)

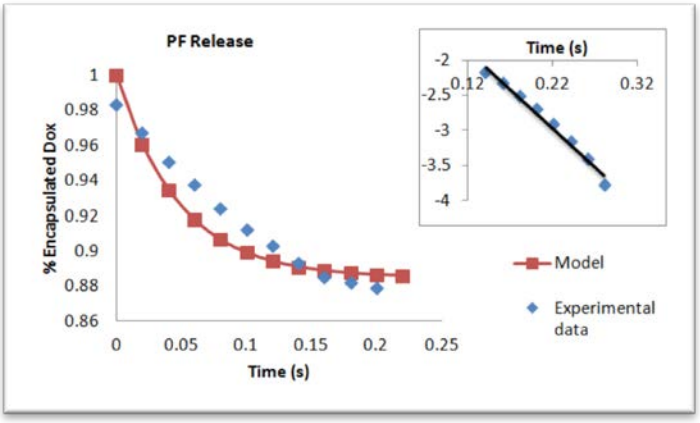

b)

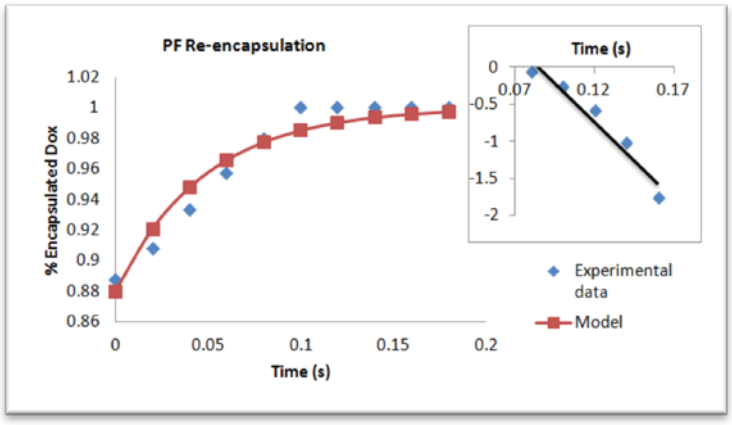

Figure 7. Typical a) release and b) re-encapsulation data from the experiment with folated micelles at 2.55 W/cm^2. The solid line is the model fit. The inserts are log transforms of the data and the model fit.

a)

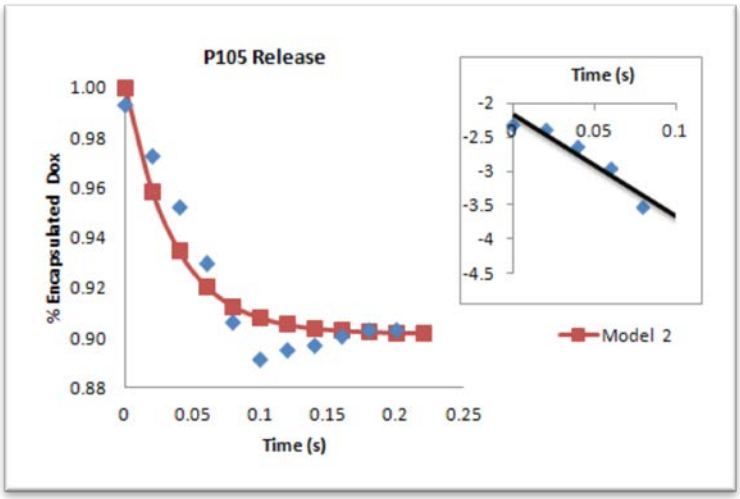

b)

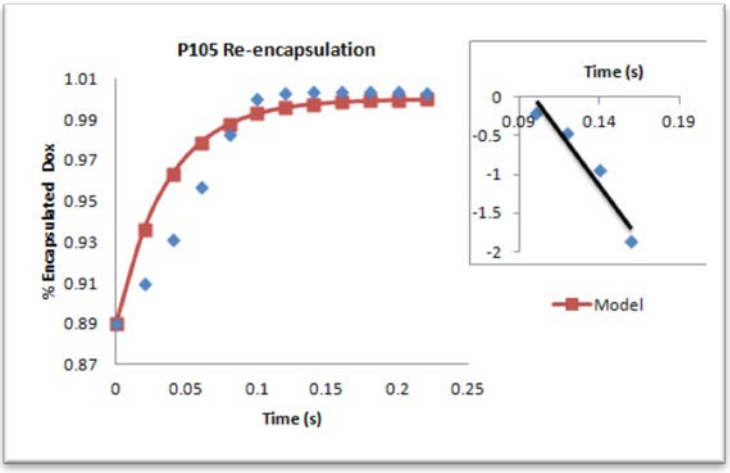

Figure 8. Typical a) release and b) re-encapsulation data from the experiment with non-folated micelles at 3.54 W/cm^2. The solid line is the model fit. The inserts are log transforms of the data and the model fit.

5.4 Acoustic Activation Power Density and Gibbs Free Energy

Fig. 9 depicts the physical meaning of activation power density. To obtain the acoustic activation power density, the Arrhenius form is used:

$$k_r = Ae^{-PD_a/PD} \tag{5-39}$$

Where k_r is the zero-order release rate constant, A is the pre-exponential factor, PD is the power density and PD_a is the acoustic activation power density.

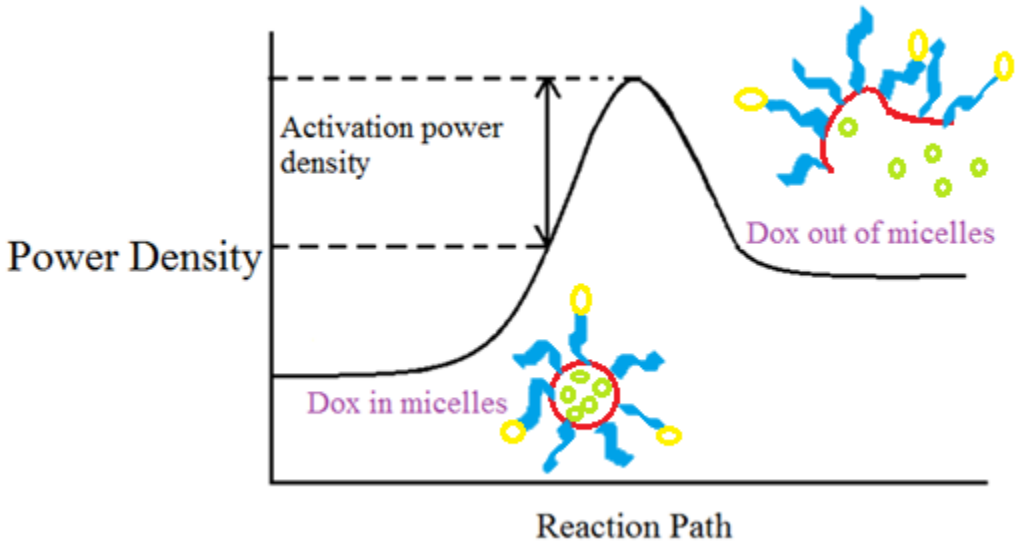

Figure 9. Plot showing the activation power density necessary to release encapsulated Dox from micelles.

Thus, a plot of $\ln(k_r)$ against 1/PD, with PD being the power density, would yield a slope that corresponds to $-PD_a$, or the negative of the acoustic activation power density, and the logarithm of the Arrhenius pre-exponential factor from the intercept. The plot is shown in Fig. 10.

a)

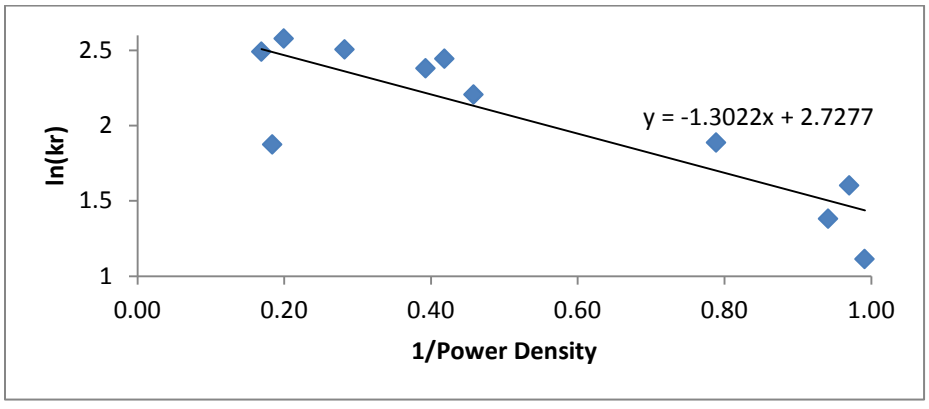

b)

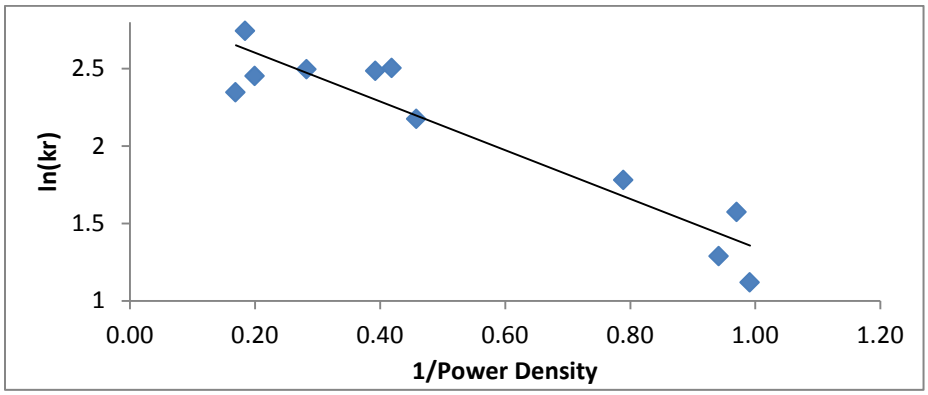

Figure 10. Plots used to find the acoustic activation power density for release for a) folated micelles and b) non-folated micelles

Table 2. Summary of results

	Acoustic Activation Power Density (W/cm^2)	Pre-Exponential Factor (μg/ml.s)
PF	1.30	15.30
P105	1.57	18.47

The Gibbs free energy is given by:

$$\Delta G = -RT\ lnK_{eq} = -RT\ ln\frac{k_r}{k_e} \tag{5-40}$$

Thus for folated micelles, $k_r = 15.30e^{-1.30/PD}$. Since k_e is almost constant (see Appendix), it is averaged over all power densities ($\bar{k}_e$). Thus, the Gibbs free energy for each power density is calculated by:

$$\Delta G = -RT \ln\left[\frac{15.30e^{-\frac{1.30}{PD}}}{\bar{k}_e}\right] \tag{5-41}$$

The Gibbs free energy obtained from the model for both folated and non-folated micelles is plotted and compared to the values given by the data. The results are shown in Fig. 11 and the model agrees with the data well.

a)

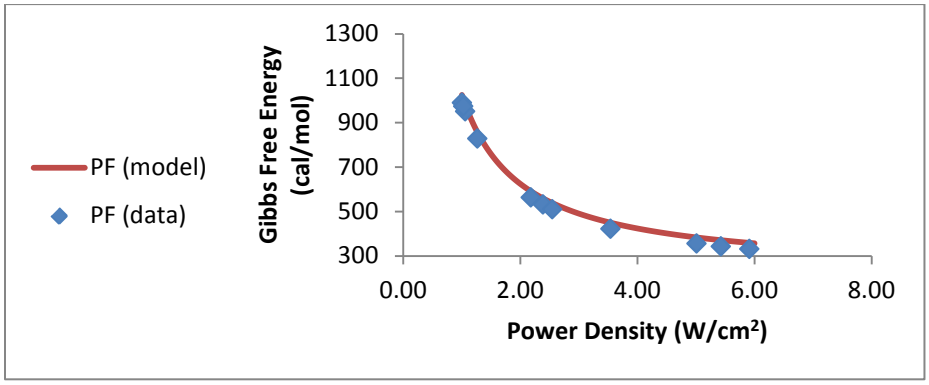

b)

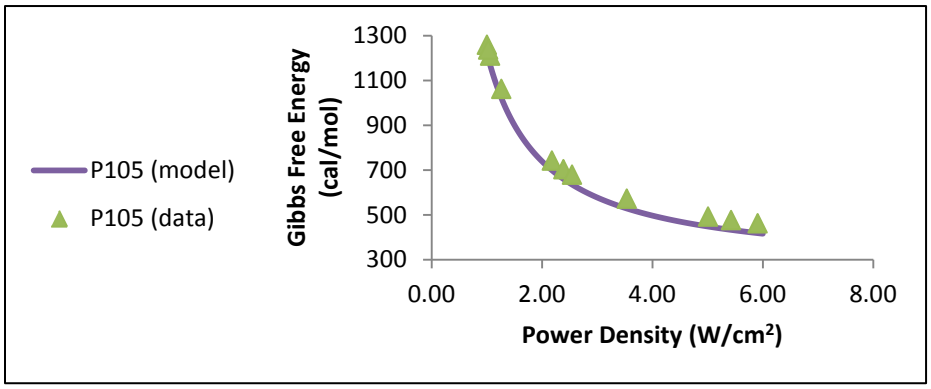

Figure 11. Plots showing the Gibbs free energy as a function of power density for a) folated micelles and b) non-folated micelles.

Chapter 6: Modeling Dox Release Using an Artificial Neural Network

An Artificial Neural Network (ANN) is a computational, mathematical model that was created based on the structure of the biological neural networks. The model is made up of a network of neurons that serve as modeling tools for non-linear statistical data. The ANN is used to model the relationship between certain inputs and outputs and sometimes to discern data patterns. This chapter covers the artificial neural network (ANN) model that was developed in an attempt to model the dynamic release of Dox from both folated and non-folated micelles and its subsequent re-encapsulation under various ultrasonic power densities at 70 kHz.

The process of drug release from micelles is highly nonlinear and a linear model would not suffice for the transient processes of release and re-encapsulation. Normally, to develop a model that would predict drug release behavior, the mechanism of the process needs to be known. However, the ANN model does not require information about the mechanism as an input. Rather, only the input and output data are needed for the process. Furthermore, the ANN model is inherently simple and has a high prediction performance [61].

The input and output data are used to first train the neurons and then to validate and test the ANN model. A feedforward ANN with one hidden layer and output feedback was developed. The structure of the network is shown in Fig. 12. The structure of the network was determined based on selecting the number of neurons in the hidden layer and training the network. The regression was then plotted and, if the data fit was poor, a different number of neurons was selected and re-trained until the best regression was obtained. The hidden layer uses the hyperbolic tangent sigmoid transfer function as the activation function and the output layer is made up of a linear neuron. Two process outputs, one current and one past, were used because the system variables (power intensity and percent encapsulated drug) vary with time. The input and target data not normalized as the neuron training yielded good results without normalization. The ANN training optimizes the model by minimizing the prediction error (or mean square errors)

between the actual fraction of encapsulated drug and the fraction predicted by the network. The final network consisted of one hidden layer with 10 neurons.

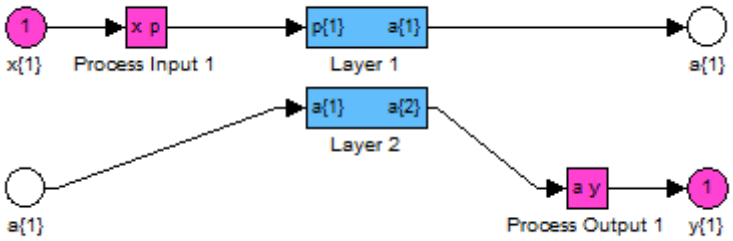

Figure 12. Network structure as shown by SimuLink.

The ANN network was simulated using MATLAB, which uses the Levenberg-Marquardt back-propagation optimization algorithm. The folated and non-folated input and output data sets were divided into three subsets, with 30% used for training, 35% for validation and another 35% for testing. The total number of data points was 12610. For folated micelles, the mean square errors for the three subsets mentioned above were 3.69582^{-5}, 3.99074^{-5}, and 3.32023^{-5}, respectively. For non-folated micelles, the errors were 3.01594^{-5}, 3.13344^{-5}, and 3.21246^{-5}, respectively. The regression in both cases was around 0.99 as can be seen in Fig. 13 and Fig. 14. It must be noted that the ANN function in MATLAB only performs well when the number of data points is large.

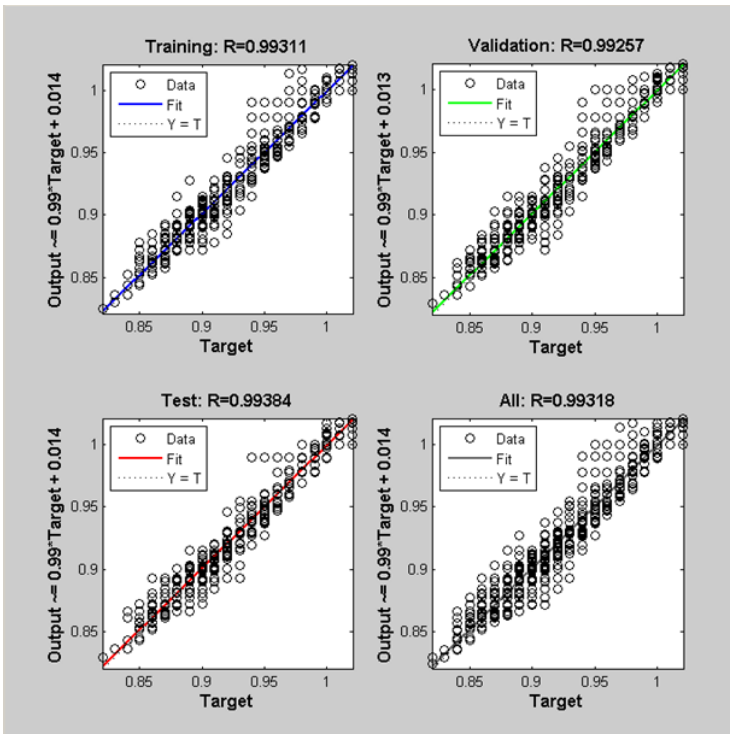

Figure 13. Regression results from the best trained ANN for folated micelles.

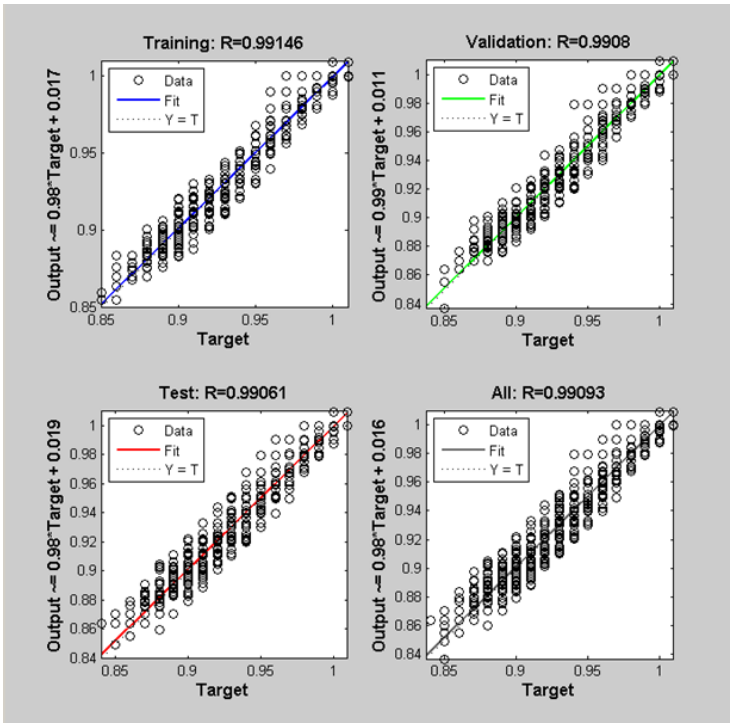

Figure 14. Regression results from the best trained ANN for non-folated micelles.

To test the predictive capabilities of the ANN, a SimuLink diagram was generated and various power densities were entered as the input. The diagram is shown in Fig. 15. The output was a very accurately predicted encapsulated Dox fraction for both types of micelles. The deviation between model predictions and the experimental data was found to be very small.

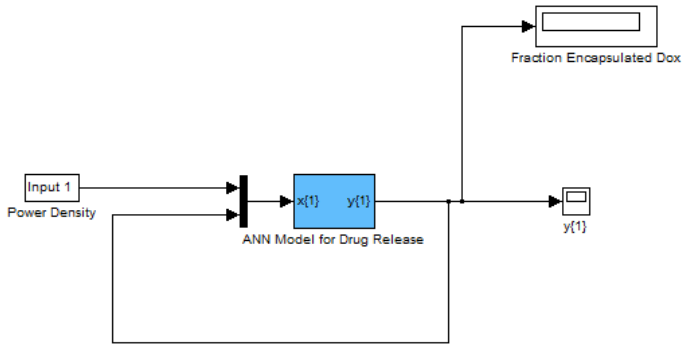

Figure 15. SimuLink diagram used to test the ANN model's predictive capabilities.

Chapter 7: Conclusion

Conventional chemotherapy as a form of cancer treatment poses many unwanted side effects since the drug is delivered systemically and affects various healthy cells as well as the target cancerous ones. One solution is to sequester the chemotherapy drug inside a polymeric micelle that would be delivered systemically as well, but which would only release its contents upon the provision of an external stimulus such as ultrasound. In this study, experimental data for ultrasonic drug release from Pluronic P105 micelles with and without an attached folic acid ligand was used.

This work explained the need for nanocarriers as a drug delivery mechanism and discussed the materials and methods involved in the preparation of the folated micelle used in the study. The release and subsequent re-encapsulation of the drug from micelles was tested at different ultrasonic power densities at 70 kHz. Furthermore, data analysis was carried out to prove that a folic acid ligand attached to a micelle does indeed contribute to greater drug release upon the provision of an acoustic stimulus. The data showed a power density threshold, below which no release occurs. The presence of this threshold suggests that transient cavitation plays an important role in drug release from micelles. An extensive review of pertinent literature was provided and the data was fitted according to two available mathematical models in order to find one which provided the best fit. The zero-order release and first-order re-encapsulation model was found to best fit the kinetic data. It was found that by fitting the data according to the models, an acoustic activation power density could be determined and the Gibbs free energy reported. Finally, an artificial neural network (ANN) model was developed to model the release and re-encapsulation of the drug and its predictive capabilities tested.

References

[1] G.A. Husseini, W.G. Pitt, The use of ultrasound and micelles in cancer treatment, J. Nanosci. Nanotechnol. 8(5) (2008) 1-11.

[2] G.A. Husseini, W.G. Pitt, Ultrasonic-activated micellar drug delivery for cancer treatment, Journal of Pharmaceutical Sciences 9999 (2008) 1-17.

[3] G.A. Husseini, N.M. Abdel-Jabbar, F.S. Mjalli, W.G. Pitt, A. Al-Mousa, Optimizing the use of ultrasound to deliver chemotherapeutic agents to cancer cells from polymeric micelles, Journal of the Franklin Institute 348 (2011) 1276-1284.

[4] H. Zhang, H. Xia, J. Wang, Y. Li, High intensity focused ultrasound-responsive release behavior of PLA-b-PEG copolymer micelles. Journal of Controlled Release 139(1) (2009) 31-39.

[5] J.R. Eisenbrey, O.M. Burstein, R. Kambhampati, F. Forsberg, J.B. Liu, M.A Wheatley, Development and optimization of a doxorubicin loaded poly(lactic acid) contrast agent for ultrasound directed drug delivery, Journal of Controlled Release 143 (2010) 38-44.

[6] M. Gou et al., Self-assembled hydrophobic honokiol loaded MPEG-PCL diblock copolymer micelles, Pharmaceutical Research 26(9) (2009) 2164.

[7] N. Munshi, N. Rapoport, W.G. Pitt, Ultrasonic activated drug delivery from Pluronic P-105 micelles, Cancer Letters 118 (1997) 13-19.

[8] G.A. Husseini, R.I. El-Fayoumi, K.L. O'Neill, N.Y. Rapoport, W.G. Pitt, DNA damage induced by micellar-delivered doxorubicin and ultrasound: comet assay study, Cancer Letters 154 (2000) 211-216.

[9] G. Husseini, D.A. Christensen, N.Y. Rapoport, W.G. Pitt, Ultrasonic release of doxorubicin from Pluronic P-105 micelles stabilized with an interpenetrating network of N,N-diethylacrylamide, Jounral of Controlled Release 83 (2002) 303-305.

[10] E.V. Batrakova, H.Y. Han, D.W. Miller, A.V. Kabanov, Effects of pluronic P85 unimers and micelles and drug permeability in polarized BBMEC and Caco-2 cells, Pharm. Res. 15 (1998) 1525.

[11] A.V. Kabanov et al., Micelle formation and solubilization of fluorescent probes in poly(oxyethylene-b-oxypropylene-b-oxyethylene) solutions, Macromolecules 28 (1995) 2303.

[12] A.V. Kabanov, V.Y. Alakhov, Pluronic block copolymers in drug delivery from micellar nanocontainers to biological response modifiers, Critical Reviews in Therapeutic Drug Carrier Systems 19(1) (2002) 1-73.

[13] N.Y. Rapoport, D.A. Christensen, H.D. Fain, L. Barrows, Z. Gao, Ultrasound-triggered drug targeting of tumors in vitro and in vivo, Ultrasonics 42 (2004) 943-950.

[14] G.A. Husseini, G.D. Myrup, W. G. Pitt, D.A. Christensen, N.Y. Rapoport, Factors affecting acoustically triggered release of drugs from polymeric micelles, Journal of Controlled Release 69 (2000) 43-52.

[15] N. Rapoport, N. Munshi, L. Pitina, W.G. Pitt, Pluronic micelles as vehicles for tumor-specific delivery of two anticancer drugs to HL-60 cells using acoustic activation, Polymer Preprints 38(1997) 620-621.

[16] N. Rapoport, Stabilization and activation of Pluronic micelles for tumor-targeted drug delivery, Colloids and Surfaces B: Biointerfaces 3 (1999) 93-111.

[17] N. Rapoport, L. Pitina, Intracellular distribution and intracellular dynamics of a spin-labeled analogue of doxorubicin by fluorescence and EPR spectroscopy, J. Pharm. Sci. 87 (1998) 321-325.

[18] N.Y. Rapoport, J.N. Herron, W.G. Pitt, L. Pitina, Micellar delivery of doxorubicin and its paramagnetic analog, ruboxyl, to HL-60: effect of micelle structure and ultrasound on the intracellular drug uptake, Journal of Controlled Release 58 (1999), 153-162.

[19] N. Rapoport, A. Marin, Md. Muniruzzaman, Micellar drug delivery to drug resistant cells using ultrasonic activation, Polymeric Materials: Science & Engineering 84 (2001) 970-971.

[20] N. Rapoport et al., Ultrasound-mediated tumor imaging and nanotherapy using drug loaded, block copolymer stabilized perfluorocarbon nanoemulsions, Journal of Controlled Release 153(1) (2011) 4-15.

[21] B. Stella et al., Design of folic acid-conjugated nanoparticles for drug targeting, Journal of Pharmaceutical Sciences 89(11) (2000) 1452-1464.

[22] R.J. Lee, P.S. Low, Folate-mediated tumor cell targeting of liposome-entrapped doxorubicin in vitro, Biochimica et Biophysica Acta 1233 (1995) 134-144.

[23] A. Gabizon, H. Shmeeda, A.T. Horowitz, S. Zalipsky, Tumor cell targeting of liposome-entrapped drugs with phospholipid-anchored folic acid- PEG conjugates, Advanced Drug Delivery Reviews 56 (2004) 1177-1192.

[24] J.M. Saul, A. Annapragada, J.V. Natarajan, R.V. Bellamkonda, Controlled targeting of liposomal doxorubicin via the folate receptor in vitro, Journal of Controlled Release 92 (2003) 49-67.

[25] N.V. Nukolova, H.S. Oberoi, S.M. Cohen, A.V. Kabanov, T.K. Bronich, Folate-decorated nanogels for targeted therapy of ovarian cancer, Biomaterials (2011) 1-10.

[26] N. Rapoport, Physical stimuli-responsive polymeric micelles for anti-cancer drug delivery, Prog. Polym. Sci. 32 (2007) 962-990.

[27] D. Chen, J. Wu, An in vitro feasibility study of controlled drug release from encapsulated nanometer liposomes using high intensity focused ultrasound, Ultrasonics 50(8) (2010) 744-749.

[28] N. Rapoport, Combined cancer therapy by micellar-encapsulated drug and ultrasound, International Journal of Pharmaceutics 277 (2004) 155-162.

[29] J.D. Pruitt, G. Husseini, N. Rapoport, W.G. Pitt, Stabilization of pluronic P-105 micelles with an interpenetrating network of N,N-Diethylacrylamide, Macromolecules 33 (2000) 9306-9309.

[30] Wang, M. Pelletier, H. Zhang, H. Xia, Y. Zhao, High-frequency ultrasound-responsive block copolymer micelle, Langmuir 25(22) 13201-13205.

[31] A. Marin, H. Sun, G.A. Husseini, W.G. Pitt, D.A. Christensen, N.Y. Rapoport, Drug delivery in pluronic micelles: effect of high-frequency ultrasound on drug release from micelles and intracellular uptake, Journal of Controlled Release 84 (2002) 39-47.

[32] G.A. Husseini, N.Y. Rapoport, D.A. Christensen, J.D. Pruitt, W.G. Pitt, Kinetics of ultrasonic release of doxorubicin from pluronic P105 micelles, Colloids and Surfaces B 24 (2002) 253-264.

[33] D. Stevenson-Abouelnasr, G.A. Husseini, W.G. Pitt, Further investigation of the mechanism of doxorubicin release from P105 micelles using kinetic models, Colloids and Surfaces B: Biointerfaces 55 (2007) 59-66.

[34] G.A. Husseini, W.G. Pitt, D.A. Christensen, D.J. Dickinson, Degradation kinetics of stabilized Pluronic micelles under the action of ultrasound, Journal of Controlled Release 138 (2009) 45-48.

[35] G. Myhr, J. Moan, Synergistic and tumour selective effects of chemotherapy and ultrasound treatment, Cancer Letters 232 (2006) 206-213.

[36] G.A Husseini et al., Kinetics of acoustic release of doxorubicin from stabilized and unstabilized micelles and the effect of temperature, Journal of the Franklin Institute 348(1) (2009) 125-133.

[37] G.A. Husseini, W.G. Pitt, D.A. Christensen, D.J. Dickinson, Degradation kinetics of stabilized Pluronic micelles under the action of ultrasound, Journal of Controlled Release 138 (2009) 45-48.

[38] G.A. Husseini, D. Stevenson-Abouelnasr, W.G. Pitt, K.T. Assaleh, L.O. Farahat, J. Fahadi, Kinetics and thermodynamics of acoustic release of doxorubicin from non-stabilized polymeric micelles, Colloids and Surfaces A: Physiochem. Eng. Aspects 359 (2010) 18-24.

[39] A. Schroeder, J. Kost, Y. Barenholz, Ultrasound, liposomes, and drug delivery: principles for using ultrasound to control the release of drugs from liposomes, Chemistry and Physics of Lipids 162 (2009) 1-16.

[40] G.A. Husseini, F.S. Mjalli, W.G. Pitt, N.M. Abdel-Jabbar, Using artificial neural networks and model predictive control to optimize acoustically assisted doxorubicin release from polymeric micelles, Technology in Cancer Research and Treatment 8 (6) (2009) 479-488.

[41] F. Mjalli, N. Abdel-Jabbar, Control of Scheibel extraction contactors using neural network based control algorithms, Industrial & Engineering Chemistry Research 44 (7) (2005) 2125-2133.

[42] J. Saint-Donat, N. Bhat, T.J. McAvoy, Neural net based model predictive control, International Journal of Control 54 (6) (1991) 1453-1468.

[43] G.A. Husseini, N.M. Abdel-Jabbar, F.S. Mjalli, W.G. Pitt, Modeling and sensitivity analysis of acoustic release of doxorubicin from unstabilized pluronic P105 using an artificial neural network model, Technology in Cancer Research and Treatment 6 (1) (2007) 49-56.

[44] K. Tachibana, T. Uchida, K. Tamura, H. Eguchi, N. Yamashita, K. Ogawa, Enhanced cytotoxic effect of Ara-C by low intensity ultrasound to HL-60 cells, Cancer Lett. 149 (2000) 189-194.

[45] Tachibana, T. Uchida, K. Ogawa, N. Yamashita, K. Tamura, Induction of cell-membrane porosity by ultrasound, Lancet 353 (1999) 1409

[46] P. Loverock, G. Ter Haar, M.G. Ormerod, P.R. Imrie, The effect of ultrasound on the cytotoxicity of adriamycin, Br. J. Radiol. 63 (1990) 542-546.

[47] B.J. Staples et al, Role of frequency and mechanical index in ultrasonic-enhanced chemotherapy in rats, Cancer Chemother. Pharmacol. 64 (2009) 593-600.

[48] J.L. Nelson, B.L. Roeder, J.C. Carmen, F. Roloff, W.G. Pitt, Ultrasonically activated chemotherapeutic drug delivery in a rat model, Cancer Research 62 (2002) 7280-7283.

[49] B.J. Staples et al., Distribution of doxorubicin in rats undergoing ultrasonic drug delivery, Journal of Pharmaceutical Sciences 99 (7) (2010) 3122-3131.

[50] N. Rapoport, D.A. Christensen, H.D. Fain, L. Barrows, and Z. Gao, Ultrasound-triggered drug targeting to tumors in vitro and in vivo. Ultrasonics 42 (2004) 943-950.

[51] G.A. Husseini, “Acoustically activated delivery of anthracycline drugs to human leukemia (HL-60) cells from Pluronic P105 micelles,” Ph.D. dissertation, Dept. Chem. Eng., Brigham Young Univ., Provo, UT, 2001.

[52] M. Muniruzzaman et al., Intracellular uptake of pluronic copolymer: effects of the aggregation state, Colloids and Surfaces B: Biointerfaces 25 (2002) 233-241.

[53] G.A. Husseini, C.M. Runyan, W.G. Pitt, Investigating the mechanism of acoustically activated uptake of drugs from Pluronic micelles, BMC Cancer 2 (2002) 1-6.

[54] S.B. Stringham et al., Over-pressure suppresses ultrasonic-induced drug uptake, Ultrasound in Med. & Biol. 35 (3) (2009) 409-415.

[55] G.A. Husseini, M.A. Diaz de la Rosa, E.S. Richardson, D.A. Christensen, W.G. Pitt, The role of cavitation in acoustically activated drug delivery, Journal of Controlled Release 107 (2005) 253-261.

[56] G.A. Husseini, K.L. O’Neill, W.G. Pitt, The comet assay to determine the mode of cell death for the ultrasonic delivery of doxorubicin to human leukemia (HL-60 cells) from Pluronic P105 micelles, Technology in Cancer Research &Treatment 4 (2005) 707-711.

[57] S. Huang, S. Sun, T. Feng, K. Sung, W. Lui, L. Wang, European Journal of Pharmaceutical Sciences, 38 (2009) 64-73.

[58] G.A. Husseini, G. D. Myrup, W. G. Pitt, D.A. Christensen, N. Y. Rapoport, Journal of Controlled Release, 69 (2000) 43-51.

[59] G.A. Husseini, M.A. Diaz, E.S. Richardson, D.A. Christensen, W.G. Pitt, The role of cavitation in acoustically activated drug delivery, J. Controlled Release 107 (2005) 253-261.

[60] G.A. Husseini, M.A. Diaz, Y. Zeng, D.A. Christensen, W.G. Pitt, Release of doxorubicin from unstabilized and stabilized micelles under the action of ultrasound, Journal of Nanoscience and Nanotechnology 7 (2007) 1-6.

[61] Bhat, N., McAvoy, T. J. Use of Neural Nets for Dynamic Modeling and Control of Chemical Process Systems, Computers & Chemical Engineering 14(4-5) (1990) 573-583.

Appendix

Table A 1 Summary of results used to obtain the acoustic activation power density and the Gibbs free energy for folated micelles.

Power Density (W/cm2)	1/PD (cm2/W)	ke (from Model 1)	avg R	kr (from Model 2)
1.01	**0.99**	**20.00**	**0.03**	**3.05**
1.06	**0.94**	**23.69**	**0.04**	**3.98**
1.03	0.97	22.20	0.05	4.96
1.27	0.79	21.98	0.07	6.60
2.18	0.46	21.38	0.09	9.08
2.39	0.42	23.68	0.11	11.51
2.55	0.39	20.83	0.12	10.80
3.54	0.28	21.20	0.13	12.24
5.01	0.20	23.89	0.12	13.16
5.43	0.18	10.07	0.14	6.52
5.91	0.17	21.18	0.13	12.04

Table A 2 Summary of results used to obtain the acoustic activation power density and the Gibbs free energy for non-folated micelles.

Power Density (W/cm2)	1/PD (cm2/W)	ke (from Model 1)	avg R	kr (from Model 2)
1.01	**0.99**	**30.27**	**0.02**	**3.06**
1.06	**0.94**	**27.66**	**0.03**	**3.63**
1.03	0.97	28.48	0.04	4.82
1.27	0.79	24.49	0.05	5.93
2.18	0.46	26.57	0.07	8.79
2.39	0.42	30.79	0.09	12.23
2.55	0.39	30.32	0.09	12.00
3.54	0.28	27.38	0.10	12.12
5.01	0.20	26.41	0.10	11.60
5.43	0.18	31.86	0.11	15.53
5.91	0.17	23.16	0.10	10.45

Vita

Laura Kherbeck was born on December 30, 1988, in Sevastopol, Ukraine. She grew up in Saudi Arabia and moved to the United Arab Emirates for high school. She graduated from the International School of Choueifat, Sharjah, as class valedictorian in 2006 and enrolled at the American University of Sharjah (AUS) that same year. She graduated from AUS in 2010. Her degree was a Bachelor of Science in Chemical Engineering.

Ms. Kherbeck began a Master's program in Chemical Engineering at the American University of Sharjah in 2010. She worked as a graduate teaching assistant for two years before graduating with a Master of Science degree in Chemical Engineering in 2012.

Laura Kherbeck has co-authored several academic publications.